

Treatment of type 2 diabetes with the designer cytokine IC7Fc

Maria Findeisen^{1,15}, Tamara L. Allen^{2,15}, Darren C. Henstridge², Helene Kammoun², Amanda E. Brandon^{1,3}, Laurie L. Baggio⁴, Kevin I. Watt⁵, Martin Pal^{1,6}, Lena Cron¹, Emma Estevez¹, Christine Yang², Greg M. Kowalski^{2,7}, Liam O'Reilly¹, Casey Egan⁸, Emily Sun⁹, Le May Thai¹, Guy Krippner², Timothy E. Adams¹⁰, Robert S. Lee², Joachim Grötzinger¹¹, Christoph Garbers¹², Steve Risis², Michael J. Kraakman², Natalie A. Mellet², James Sligar¹, Erica T. Kimber¹, Richard L. Young¹³, Michael A. Cowley¹⁴, Clinton R. Bruce^{2,7}, Peter J. Meikle², Paul A. Baldock¹, Paul Gregorevic⁵, Trevor J. Biden¹, Gregory J. Cooney^{1,3}, Damien J. Keating⁹, Daniel J. Drucker⁴, Stefan Rose-John¹¹ & Mark A. Febbraio^{1,2,8*}

The gp130 receptor cytokines IL-6 and CNTF improve metabolic homeostasis but have limited therapeutic use for the treatment of type 2 diabetes. Accordingly, we engineered the gp130 ligand IC7Fc, in which one gp130-binding site is removed from IL-6 and replaced with the LIF-receptor-binding site from CNTF, fused with the Fc domain of immunoglobulin G, creating a cytokine with CNTF-like, but IL-6-receptor-dependent, signalling. Here we show that IC7Fc improves glucose tolerance and hyperglycaemia and prevents weight gain and liver steatosis in mice. In addition, IC7Fc either increases, or prevents the loss of, skeletal muscle mass by activation of the transcriptional regulator YAP1. In human-cell-based assays, and in non-human primates, IC7Fc treatment results in no signs of inflammation or immunogenicity. Thus, IC7Fc is a realistic next-generation biological agent for the treatment of type 2 diabetes and muscle atrophy, disorders that are currently pandemic.

Type 2 diabetes (T2D) is highly prevalent, with an estimated 370 million affected individuals worldwide, and this is predicted to double by 2030^{1,2}. Despite the presence of several well-established drug classes for treating T2D, there is still a considerable unmet need for a drug that halts or reverses disease progression. The gp130 receptor cytokines IL-6 and CNTF modify food intake and body weight and improve insulin resistance in mice and humans^{3–6}. Axokine, the human variant of CNTF, underwent human clinical trials for the treatment of amyotrophic lateral sclerosis, but the drug was repurposed to treat obesity and T2D^{7–9}. After showing promise, the clinical development of Axokine was discontinued when some treated patients developed antibodies⁹, because of the fear that this could interfere with the neuroprotective action of endogenous CNTF. Although IL-6 protects against obesity and insulin resistance¹⁰, it is also pro-inflammatory owing—in part—to its ‘trans-signalling’ effects^{11,12}, which limits its therapeutic utility.

The gp130 cytokines signal by binding to the cytokine α -receptors, which are the IL-6 receptor (IL-6R) and CNTF receptor (CNTFR) for IL-6 and CNTF, respectively. Binding initiates the recruitment and dimerization of two transmembrane β -receptors: the IL-6-IL-6R complex binds two gp130 receptors as a homodimer, whereas the CNTF-CNTFR complex binds gp130 receptor and the LIF receptor (LIFR) as a heterodimer¹³. By transferring the LIFR-binding module from CNTF to IL-6, we engineered the chimeric protein IC7¹⁴, which predominantly consists of IL-6 residues, rendering it far less likely to induce an immune response compared with CNTF, because IL-6 circulates freely whereas CNTF is intracellular, and lacks a signal sequence peptide. Because IC7 is a chimaera with a unique sequence

and structure, any neutralizing antibodies against it will be less likely to interfere with endogenous protein action. Here we show that a modification of IC7 (namely, IC7Fc) improves glucose tolerance, prevents weight gain and liver steatosis in obese mice. Moreover, IC7Fc has a marked capacity to maintain muscle mass in circumstances in which untreated animals lose muscle or, indeed, to increase muscle mass. Notably, in studies in non-human primates, we show that the drug is safe, without any adverse events, has no adverse toxicology and no signs of immunogenicity.

IC7 can bind and signal

Figure 1a and Extended Data Fig. 1a depict the module swap and epitope shuffling that result in the formation of IC7 and IC7Fc, which contain the site III from CNTF (Fig. 1a, orange) with the remainder IL-6 (Fig. 1a, grey), resulting in signalling that is different from any endogenous gp130 receptor ligand. IC7 competitively inhibited labelled IL-6 and displayed comparable affinity to the IL-6R (Extended Data Fig. 1c). When secreted into the bloodstream, IL-6 binds to the soluble IL-6R, and the resulting complex will bind to soluble gp130 and thereby be neutralized¹². IC7 binds to the soluble IL-6R, but the complex of IC7 and soluble IL-6R is not neutralized by soluble gp130, owing to the presence of a LIFR-binding site in IC7 (Extended Data Fig. 1b). IL-6-induced phosphorylation of STAT3 was reduced by the addition of soluble IL-6R but no such reduction was observed for IC7 (Extended Data Fig. 1b), which indicates that—unlike IL-6—IC7 is not buffered in these circumstances. IL-6 induces the synthesis of haptoglobin in hepatocytes, during the acute-phase response¹⁵. IC7 also increased the

¹The Garvan Institute of Medical Research, Sydney, New South Wales, Australia. ²Baker Heart & Diabetes Institute, Melbourne, Victoria, Australia. ³Charles Perkins Centre, University of Sydney, Sydney, New South Wales, Australia. ⁴Department of Medicine, Lunenfeld Tanenbaum Research Institute, Mount Sinai Hospital, University of Toronto, Toronto, Ontario, Canada. ⁵Centre of Muscle Research, Department of Physiology, The University of Melbourne, Melbourne, Victoria, Australia. ⁶Walter and Eliza Hall Institute of Medical Research, Department of Medical Biology, The University of Melbourne, Melbourne, Victoria, Australia. ⁷Institute for Physical Activity and Nutrition, Deakin University, Melbourne, Victoria, Australia. ⁸Monash Institute of Pharmaceutical Sciences, Monash University, Melbourne, Victoria, Australia. ⁹Molecular & Cellular Physiology Laboratory, Flinders University, Adelaide, South Australia, Australia. ¹⁰CSIRO Manufacturing, Melbourne, Victoria, Australia. ¹¹Department of Biochemistry, Christian-Albrechts-Universität zu Kiel, Kiel, Germany. ¹²Institut für Pathologie, Otto von Guericke University, Magdeburg, Germany. ¹³Adelaide Medical School, University of Adelaide, Adelaide, South Australia, Australia. ¹⁴Department of Physiology, Monash University, Melbourne, Victoria, Australia. ¹⁵These authors contributed equally: Maria Findeisen, Tamara L. Allen. *e-mail: mark.feelb@monash.edu

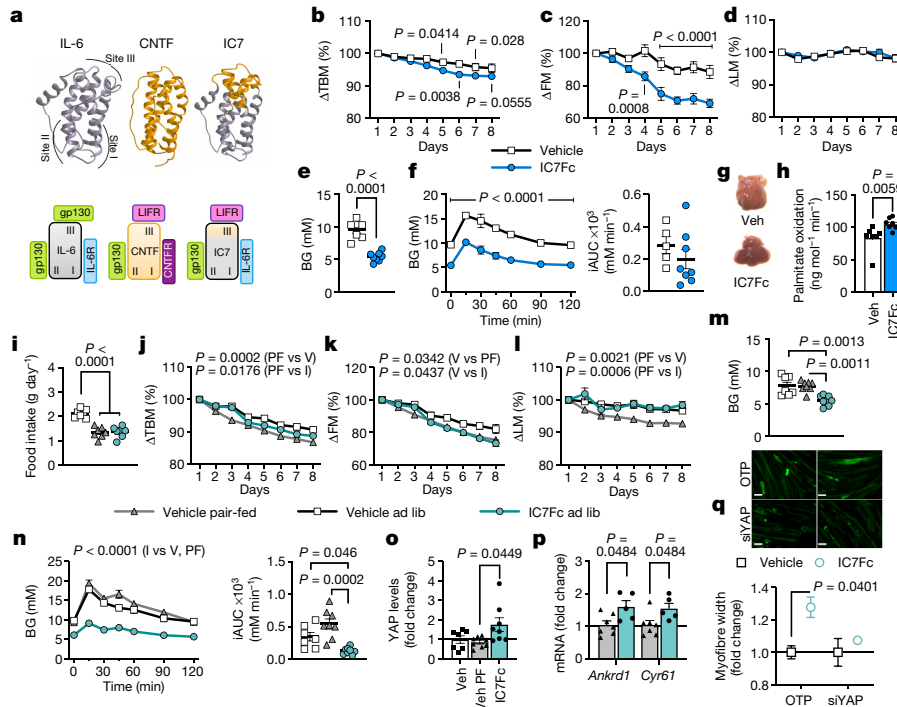


Fig. 1 | IC7Fc improves metabolism in DIO mice. **a**, Schematic model of IC7. **b–h**, DIO mice injected daily for 7 days with vehicle ($n = 7$, 5 in **f**) or IC7Fc (1 mg kg^{-1} , $n = 8$). The percentage change in total body mass (TBM, **b**), fat mass (FM, **c**), and lean mass (LM, **d**) were determined. Fasting blood glucose (BG) levels (**e**) and glucose tolerance (**f**) were determined on day 5. Representative liver photographs ($n = 4$ per group) (**g**) and palmitate oxidation (**h**) are shown. **i–q**, Paired-feeding study. Mice were divided into the three groups: vehicle ad libitum (V) ($n = 7$); IC7Fc ad libitum (I) ($n = 8$, 7 in **j**); and vehicle pair-fed (PF) ($n = 8$, 7 in **j**). The vehicle pair-fed group commenced 1 day after the other groups. Food intake (**i**) and change in total body mass (**j**), fat mass (**k**) and lean mass (**l**) were determined. Fasting blood glucose levels (**m**) and glucose tolerance (**n**) were determined. Quantification of YAP1 protein expression (**o**) and

Ankrd1 ($n = 7$) and *Cyr61* ($n = 5$) mRNA expression (**p**) in gastrocnemius muscles. **q**, Quantification of width (bottom) and representative images of sarcomeric myosin labelling (top) from control (OTP) and YAP1 knockdown (siYAP1) C2C12 myotubes treated with vehicle or IC7Fc (1 ng ml^{-1}) for 24 h ($n = 3$). Scale bars, $10 \mu\text{m}$. Data are mean \pm s.e.m. *P* values determined by: two-way analysis of variance (ANOVA) with Sidak's multiple comparisons test (**b–d**, **f**); Student's two-tailed unpaired *t*-test (**e**); two-tailed unpaired Mann–Whitney *U*-test (**h**); multiple *t*-test using the Holm–Sidak method (**p**, **q**); one-way ANOVA with Tukey's multiple comparisons test (**i**, **m**); two-way ANOVA with Tukey's multiple comparisons test for main treatment effect (**j–l**, **n**); non-parametric Kruskal–Wallis test with Dunn's multiple comparisons test (**o**).

secretion of haptoglobin (Extended Data Fig. 1d) and phosphorylation of STAT3 (Extended Data Fig. 1e). We next fed mice a high-fat diet (HFD) for 8 weeks, and injected them with 1 mg kg^{-1} IC7 into the intraperitoneal cavity, every day for 7 days before killing on day 8. Unmodified IC7 did not have any effect on glucose tolerance compared with vehicle-injected controls (Extended Data Fig. 1f).

IC7Fc improves metabolism in obese mice

IC7 in vivo showed limited efficacy in diet-induced obese (DIO) mice, in contrast with our previous observations with IL-6 and CNTF^{3,4}; this may be due to protein pharmacokinetics. Two biopharmaceutical technologies are the covalent attachment of the polymer polyethylene glycol (PEG) to protein (PEGylation)¹⁶ and fusion with the fragment crystallizable (Fc) domain of IgG¹⁷. We generated three species of modified IC7; two linear chain PEGylated forms of IC7 (30 kDa (mIC7A) and 40 kDa (mIC7B)) and an IC7–human Fc fusion protein (IC7Fc). These had similar efficiency to IC7 in terms of receptor binding, haptoglobin secretion and STAT3 phosphorylation (Extended Data Fig. 1e, g–i). mIC7A and mIC7B also had marked effects on improving glucose tolerance in DIO mice (Extended Data Fig. 1f). IC7Fc phosphorylated STAT3 in tissues (Extended Data Fig. 1j–l) and, as predicted, improved the pharmacokinetics compared with unmodified IC7 (Extended Data Fig. 1m). We also performed dose–response and route-of-delivery optimization experiments (Extended Data Fig. 2a). We next fed mice a HFD for 8 weeks and injected them intraperitoneally with 1 mg kg^{-1} IC7Fc, or an equal volume of saline, daily for 7 days, which decreased body (Fig. 1b) and fat (Fig. 1c) mass without changing lean (Fig. 1d) mass. After 4 days, we performed intraperitoneal glucose tolerance

tests. IC7Fc markedly reduced fasting glucose levels (Fig. 1e) and improved glucose tolerance (Fig. 1f). Although the same weight, livers from vehicle-treated mice were paler than those from IC7Fc-treated mice (Fig. 1g), consistent with increased hepatosteatosis, which was accompanied by decreased palmitate oxidation in homogenates of vehicle- versus IC7Fc-treated mice (Fig. 1h). PEGylated IC7 increased AMP kinase (AMPK) activity and reduced the mRNA expression of *SREBP1c* (also known as *Srebfl1*) and *Dgat1* in liver (Extended Data Fig. 2b, c). Given the simplicity of production and purification of IC7Fc, we concentrated subsequent experiments on IC7Fc. We observed no differences in measurements when comparing IC7Fc with mIC7A or mIC7B, which suggests that the effects of IC7Fc were not due to the Fc modification per se. We next injected IC7Fc (1 mg kg^{-1}) or vehicle every other day for 16 days. IC7Fc reduced body and fat mass (Extended Data Fig. 2d, e) and maintained lean mass (Extended Data Fig. 2f). As IC7Fc caused weight loss, we assessed whether this was related to whole-body oxygen consumption (VO_2). IC7Fc indeed increased VO_2 (Extended Data Fig. 2g, h). Thus, chronic IC7Fc treatment decreases body weight, fat mass and liver steatosis via mechanisms that involve AMPK activity and increased lipid oxidation and whole-body VO_2 .

We next placed mice on a HFD for 9 weeks and during week 8, divided mice into vehicle-treated ad libitum, IC7Fc-treated daily (1 mg kg^{-1} injected intraperitoneally) and vehicle-treated 'pair-fed' groups. The latter group commenced one day after other groups to match food intake. IC7Fc decreased food intake by approximately 50% and the paired feeding was effective (Fig. 1i). The decrease in body mass was greater in the vehicle-treated pair-fed mice compared with other groups, and although IC7Fc decreased body mass relative

to vehicle-treated ad libitum mice, this decrease was not as pronounced as with the vehicle-treated pair-fed mice (Fig. 1j, Extended Data Fig. 2i). When examining the effect of treatment on loss of fat mass, it was clear that the loss in adiposity induced by IC7Fc treatment was entirely due to a decrease in food intake, because this decrease was identical to the vehicle-treated pair-fed mice (Fig. 1k, Extended Data Fig. 2i). Even though IC7Fc was matched for food intake with vehicle-treated pair-fed mice, it prevented the marked loss of lean mass seen in the pair-fed mice (Fig. 1l, Extended Data Fig. 2i). IC7Fc treatment also decreased the concentrations of triacylglycerol and diacylglycerol in the liver (Extended Data Fig. 2j). As decreased liver steatosis and fat mass are associated with improved metabolic homeostasis, we measured fasting glycaemia and glucose tolerance. Both fasting glycaemia (Fig. 1m) and glucose tolerance (Fig. 1n) were uncoupled from fat mass, because IC7Fc treatment—but not pair-fed vehicle treatment—was effective in improving glycaemia compared with mice treated with vehicle ad libitum. The observation that skeletal muscle mass was preserved in the presence of reduced nutrient intake was crucial because increased muscle mass reduces the risk of T2D¹⁸, whereas sarcopenia, a loss of muscle mass with ageing, is associated with heart failure and dementia¹⁹. Because increased gp130 signalling affects the Hippo pathway—specifically activation of the transcriptional coactivator YAP1²⁰, which can increase muscle fibre growth²¹—we hypothesized that such activation was a mechanism for the effect of IC7Fc on muscle. YAP1 protein expression (Fig. 1o), but not mRNA expression or protein phosphorylation (Ser112) (Extended Data Fig. 2k, l), was increased by IC7Fc. The mRNA expression of *Ankrd1* (also known as *Rfxank*) and *Cyr61* (*Ccn1*), downstream target genes of YAP1, was also increased by IC7Fc (Fig. 1p). Next, we knocked down YAP1 using short interfering RNA (siRNA) in myotubes of mouse C2C12 cells (Extended Data Fig. 2m), and treated the siRNA control and *Yap1* siRNA myotubes with vehicle or IC7Fc for 24 h. Myofibre width was increased by approximately 25% in the siRNA control cells treated with IC7Fc, but no such effect was seen in *Yap1* siRNA cells (Fig. 1q). Activation of YAP1 in liver causes fibrosis²². Unlike its effect in skeletal muscle, IC7Fc treatment tended to decrease the expression of YAP1 protein in the liver (Extended Data Fig. 2n). Together, IC7Fc not only improves metabolism in DIO mice but also prevents the loss of muscle mass.

We next fed mice either a chow or HFD and then acutely administered IC7Fc (1 mg kg⁻¹ intraperitoneally) or saline (vehicle) (Extended Data Fig. 3a). IC7Fc decreased blood glucose levels (Fig. 2a, Extended Data Fig. 3b), and increased levels of plasma insulin and C-peptide (Fig. 2b, Extended Data Fig. 3c, d), which suggests that it was acting as an insulin secretagogue. IC7Fc also improved glucose tolerance (Extended Data Fig. 3e), increasing insulin and C-peptide during the glucose tolerance test (Extended Data Fig. 3f, g). We next performed experiments in leptin-receptor-deficient mice (*Lepr^{db/db}*; Extended Data Fig. 3h). *Lepr^{db/db}* mice display frank hyperglycaemia at an early age (Extended Data Fig. 3i), but, similar to patients with T2D, transition from β cell compensation to failure. Although IC7Fc had similar efficacy as our DIO models in acutely lowering glucose in 7-week-old *Lepr^{db/db}* mice, this progressively diminished, such that by 17 weeks of age (when the *Lepr^{db/db}* mice displayed β cell failure) IC7Fc was no longer effective, in contrast with *Lepr^{db/+}* control mice (Fig. 2d, Extended Data Fig. 3j). Notably, a single dose of IC7Fc decreased total body and fat mass, tending to increase lean mass (Fig. 2c), and decreased fasting insulin (Fig. 2e) 10 days later—effects not observed in *Lepr^{db/+}* control mice (Extended Data Fig. 3k, l). Fasting glucose was unaffected (Extended Data Fig. 3m). We next assessed whether the acute glucose-lowering effect of IC7Fc was due to its insulinotropism, by administering the β cell toxin streptozotocin (STZ) (Extended Data Fig. 3n). By 18 days, STZ-treated mice developed frank hyperglycaemia and hyperinsulinaemia (Extended Data Fig. 3o). After 4 weeks, we performed a fasting/refeeding experiment in mice injected with IC7Fc (1 mg kg⁻¹) or saline (vehicle). IC7Fc decreased blood glucose and increased insulin in control mice but not in STZ-treated mice (Fig. 2f, Extended Data Fig. 3p), which demonstrates that the glucoregulatory effect of IC7Fc was dependent on functional β cells.

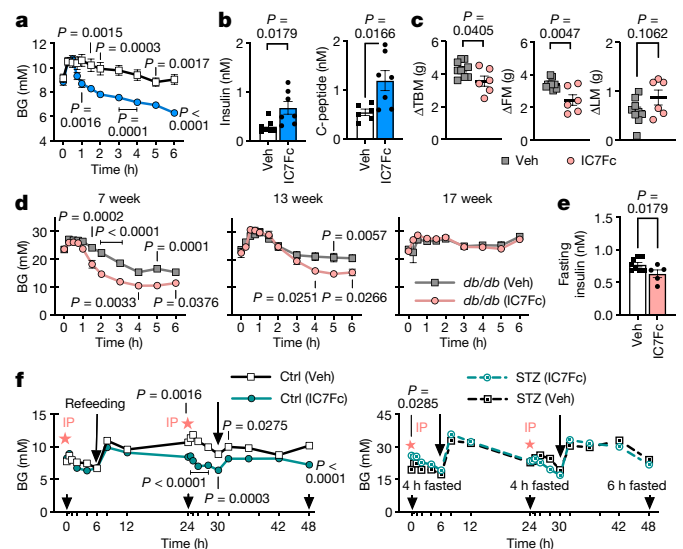


Fig. 2 | IC7Fc decreases glucose via increased insulin. **a–c**, Single intraperitoneal dose of vehicle (veh) or IC7Fc (1 mg kg⁻¹) in the fed state of HFD mice ($n = 13$). Levels of blood glucose (**a**), plasma insulin ($n = 7$) and C-peptide ($n = 6–7$) (**b**) were determined. Changes in total body, fat mass and lean mass were determined 10 days after a single dose of vehicle ($n = 9$) or IC7Fc (1 mg kg⁻¹, $n = 6$) in *Lepr^{db/db}* mice (**c**). **d**, **e**, Blood glucose levels (**d**) in 7-week (left), 13-week (middle) and 17-week (right) male *Lepr^{db/db}* (*db/db*) mice; $n = 9$ (Veh) and $n = 6$ (IC7Fc) in left panel; $n = 7$ (Veh) and $n = 8$ (IC7Fc) in middle and right panels. **e**, Fasting plasma insulin levels 17 days after treatment; $n = 8$ (Veh) and $n = 5$ (IC7Fc). **f**, Glycaemia over 48 h during a fasting/refeeding experiment in response to intraperitoneal injections of vehicle or IC7Fc (1 mg kg⁻¹). Ten-week-old male control mice treated with placebo (ctrl; left; $n = 10$) or diabetic mice induced by STZ (55 mg kg⁻¹; right; $n = 7$ for vehicle and $n = 9$ for IC7Fc). Data are mean \pm s.e.m. P values determined by: two-way ANOVA with Sidak's multiple comparisons test (**a**, **d**, **f**); or Student's two-tailed unpaired t -test (**b**, **c**, **e**).

To determine the fate of glucose in a physiologically relevant setting, we performed stable isotope tracer D-[6,6'-²H₂]glucose oral glucose tolerance tests (OGTTs) in DIO mice. IC7Fc improved glucose tolerance, decreased hepatic glucose, tracer enrichment and tracer glucose load compared with vehicle (Extended Data Fig. 4a–d). In normal circumstances, we would next perform euglycaemic–hyperinsulinaemic clamp experiments¹¹, but because we showed that IC7Fc is primarily insulinotropic, this clamp technique would demonstrate little effect of IC7Fc as insulin is matched between vehicle- and IC7Fc-treated mice, and this was the case (Extended Data Fig. 4e). Instead, we performed euglycaemic clamps in IC7Fc- or saline-treated mice (Extended Data Fig. 4f, g) in the presence or absence of octreotide—an octapeptide that mimics natural somatostatin. We successfully clamped glucose during the IC7Fc trial to vehicle, but because octreotide inhibits insulin (Extended Data Fig. 4h), such treatment slightly increased steady-state glucose levels (Fig. 3a, Extended Data Fig. 4i). Although we did not infuse any glucose in vehicle, IC7Fc required an increased glucose infusion rate (GIR) to maintain normal blood glucose levels (Fig. 3b, Extended Data Fig. 4j). The addition of octreotide with IC7Fc abolished (Fig. 3b) or reduced (Extended Data Fig. 4j) its effect on the GIR. IC7Fc markedly increased both the suppression of hepatic glucose production (Fig. 3c, Extended Data Fig. 4k) and glucose disposal (Fig. 3d, Extended Data Fig. 4l), and these effects were abrogated by octreotide. Notably, no significant IC7Fc-mediated increases in white adipose tissue, skeletal muscle or brain glucose uptake (Rg⁺) were observed (Extended Data Table 1), but instead we observed an approximately 2–4-fold increase in glucose uptake into brown adipose tissue (BAT) (Fig. 3e, Extended Data Fig. 4m), which was blunted by the addition of octreotide. Although a functional pancreas was necessary for the IC7Fc to increase the GIR, because the addition of octreotide abrogated any

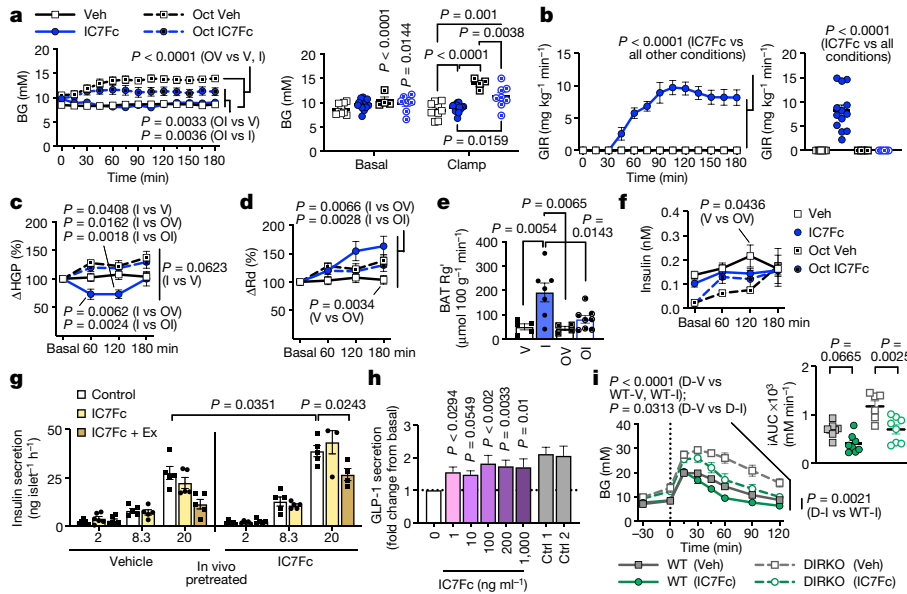


Fig. 3 | IC7F effects are pancreas-dependent but incretin-independent. **a–f**, Euglycaemic clamp studies in DIO mice treated with vehicle or IC7F (1 mg kg⁻¹), in the presence or absence of octreotide (7.5 μg kg⁻¹ min⁻¹); *n* = 9 (Veh; V), *n* = 13 (IC7F; I), *n* = 4 (Oct Veh; OV), *n* = 8 (Oct IC7F; OI). Blood glucose (**a**), the GIR (**b**), hepatic glucose production (HGP; **c**), glucose disposal (Rd; **d**), glucose uptake (Rg) in BAT (**e**), and plasma insulin (**f**) were determined before (basal) and during the clamp. **g**, GSIS from isolated islets of DIO mice intraperitoneally injected daily with vehicle or IC7F (1 mg kg⁻¹) (*n* = 10 mice per group). Stimulation with glucose doses containing saline control or 100 ng ml⁻¹ IC7F in the presence or absence of 100 nmol l⁻¹ Ex(9–39). **h**, GLP-1

secretion from human colonic mucosal tissue (*n* = 10) after treatment with IC7F and positive controls (ctrl 1: 3-isobutyl-1-methylxanthine (IBMX) and forskolin (FSK); ctrl 2: potassium). **i**, DIO double incretin receptor knockout (DIRKO) and wild-type (WT) littermate control mice treated with vehicle or IC7F (1 mg kg⁻¹) 30 min before OGTs (*n* = 6 for DIRKO Veh; *n* = 8 for all other groups). Data are mean ± s.e.m. *P* values determined by: two-way ANOVA (**a–d**, **f**, **i**) with Sidak's multiple comparisons test (**a**, **c**, **d**) or Tukey's multiple comparisons test (**a**, **b**, **f**, **i**); ordinary one-way ANOVA (**b**, **e**, **h**, **i**) with Tukey's multiple comparisons test (**b**, **e**, **i**) or uncorrected Fisher's least significant difference test (**h**); or multiple *t*-test using the Holm–Sidak method (**g**).

response (Fig. 3b, Extended Data Fig. 4j), the effects of IC7F on the GIR, hepatic glucose production and glucose turnover in the absence of octreotide were not due to increased levels of insulin per se in this model (Fig. 3f, Extended Data Fig. 4n).

IC7F acts, in part, via incretins

IC7F did not acutely affect glucose-stimulated insulin secretion (GSIS) in isolated mouse islets (Extended Data Fig. 5a). Because IL-6 increases glucagon-like peptide (GLP-1) in mice²³, we wondered whether IC7F could be activating incretins. DIO mice were intraperitoneally injected daily with vehicle or IC7F (1 mg kg⁻¹). IC7F did not acutely affect GSIS, insulin or glucagon in the islets (Fig. 3g, Extended Data Fig. 5b), but IC7F pre-treatment increased GSIS at 20 mM glucose in the absence or presence of acute IC7F (Fig. 3g), which was blunted by the GLP-1 receptor antagonist exendin-(9–39)-amide (Ex(9–39); 25 nmol kg⁻¹), implicating the GLP-1R in the insulintropic effect of IC7F. In the islet lysates, there was a non-significant increase (*P* = 0.06) in GLP-1 after IC7F treatment (Extended Data Fig. 5c). IC7F decreased glucose and increased insulin, C-peptide, glucagon, and total and active GIP (Extended Data Fig. 5d). Together, these data suggested that although IC7F increases insulin secretion, it is unlikely to lead to hypoglycaemic events because it also increases glucagon, and that incretins were implicated in the mechanism of action of IC7F. We next analysed human colonic tissue for GLP-1 secretion after treatment with IC7F. Even at the lowest dose of 1 ng ml⁻¹, IC7F treatment increased the release of GLP-1 (Fig. 3h). As IC7F activated GLP-1 and GIP, we assessed whether the mechanism of action of IC7F was by the activation of incretins, by performing OGTs in DIO mice deficient in both GLP-1R and GIPR (double incretin receptor knockout, DIRKO) and in wild-type littermate control mice. IC7F was equally effective in improving glucose tolerance when comparing the double-knockout and wild-type mice (Fig. 3i), demonstrating that although IC7F can increase incretins, the

metabolic actions of acute IC7F treatment are not entirely incretin-dependent.

IC7F transgenic mice are protected from obesity

To examine the long-term effects of IC7F on metabolism, we generated ROSA26-IC7F mice (Extended Data Fig. 6a) and crossed these with *Alb-cre* mice to generate liver-specific transgenic mice that overexpress IC7F (IC7F^{Alb-cre}) (Extended Data Fig. 6b, c) and control (IC7F^{WT}) mice. After weaning, all mice were placed on a chow diet for 6 weeks. After this period, half of the mice were switched to a HFD and all mice were monitored for an additional 6 weeks. As expected, marked phosphorylation of STAT3 in the liver was observed in IC7F^{Alb-cre} but not wild-type mice (Fig. 4a, Extended Data Fig. 6d). All mice were healthy and gained weight normally, but IC7F^{Alb-cre} mice were refractory to gaining fat mass, but not lean mass, over time (Extended Data Fig. 6e). When fed a HFD, IC7F^{Alb-cre} mice gained less body (Fig. 4b) and fat (Fig. 4c) mass, but consistent with the paired-feeding study, IC7F^{Alb-cre} mice had more lean mass (Fig. 4d). IC7F^{Alb-cre} DIO mice had improved glucose tolerance and lower levels of basal glucose, insulin, non-esterified fatty acids (NEFA) (Fig. 4e–h) and higher levels of glucagon (Fig. 4i). This phenotype was mostly matched in chow-fed mice (Extended Data Fig. 6f–i). Increased IL-6 is associated with osteoporosis²⁴. High-resolution micro-computed tomography imaging was performed on femurs from female IC7F^{Alb-cre} and wild-type mice. Consistent with the injection experiments, IC7F^{Alb-cre} mice tended (*P* = 0.06) to display higher circulating levels of GIP (Fig. 4j). GIP positively affects bone density, so it was not surprising that IC7F^{Alb-cre} mice had higher bone volume/trabecular volume ratios, less trabecular separation and greater trabecular numbers (Fig. 4k–m). The role of 'myokines' in health and disease is well established²⁵. We next determined whether IC7F overexpression, predominantly in skeletal muscle, would have the predicted phenotype by crossing our ROSA26-IC7F mice to *MCK-cre* (also known as *Ckm-cre*) mice to generate

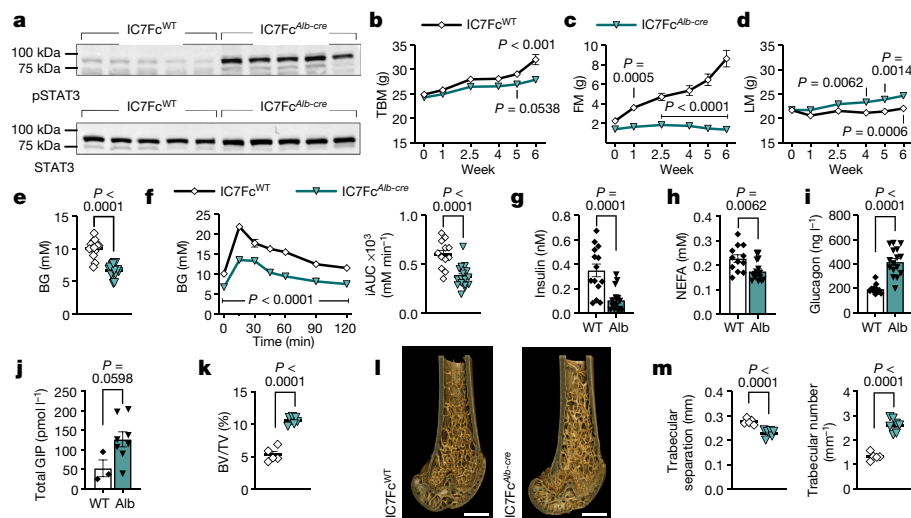


Fig. 4 | Phenotype of IC7Fc-overexpressing mice. **a–j**, Ten-week-old mice that overexpress liver-specific IC7Fc (IC7Fc^{Alb-cre}; $n = 16$) and control mice (IC7Fc^{WT}; $n = 14$) fed a HFD for 6 weeks. **a**, Liver STAT3 phosphorylation. Total body mass (**b**), fat mass (**c**) and lean mass (**d**) were determined. **e**, Blood glucose levels in control and transgenic IC7Fc^{Alb-cre} mice. **f–j**, Levels of blood glucose during an OGTT (**f**), plasma insulin (**g**), NEFA (**h**), glucagon (**i**) (in **e–h**, $n = 12$ for WT) and total GIP (**j**) ($n = 3$ for WT and $n = 8$ for *Alb-cre*). **k–m**, High-resolution micro-computed

tomography imaging on femurs from 14-week-old female IC7Fc^{AlbCre} ($n = 7$) and control ($n = 5$) mice. Percentage of the ratio of bone volume (BV) to total volume (TV) (**k**), representative Drishti 3D images of trabecular data (**l**), and quantification of trabecular separation (left) and number (right) (**m**). Scale bars, 1 mm. Data are mean \pm s.e.m. P values determined by: two-way ANOVA with Sidak's multiple comparisons test (**b–d**, **f**); Student's two-tailed unpaired t -test (**e–i**, **k**, **m**); or nonparametric two-tailed unpaired Mann–Whitney U -test (**j**).

IC7Fc^{MCK-cre} mice. The IC7Fc^{MCK-cre} mice essentially phenocopied the IC7Fc^{Alb-cre} mice (Extended Data Fig. 6j–u).

IC7Fc is a valuable add-on to existing T2D therapy

IC7Fc treatment displayed similar actions to GLP-1R agonists such as decreased food intake, weight loss and increased GSIS²⁶. Dulaglutide (trade name Trulicity) is one such agonist that, similar to IC7Fc, is covalently linked to an Fc fragment of IgG4²⁷. Dulaglutide is effective in T2D, but can have side effects including nausea, vomiting, diarrhoea and fatigue²⁸, possibly owing to hypoglycaemia. We acutely injected mice with IC7Fc, dulaglutide (GLP-1RA) or a combination of the two (Extended Data Fig. 7a). Although treatment with both IC7Fc and GLP-1RA did not affect the decrease in fat mass induced by GLP-1RA treatment, it normalized the loss of muscle mass 5–7 days after injection (Extended Data Fig. 7b). Notably, whereas GLP-1RA treatment resulted in borderline hypoglycaemia in some mice, this was not seen in the combined IC7Fc plus GLP-1RA treatment group (Extended Data Fig. 7c), possibly owing to the effects on glucagon (Extended Data Fig. 7d). IC7Fc treatment increased VO_2 , VCO_2 and substrate oxidation, as measured by the respiratory exchange ratio and total energy expenditure. Moreover, the reduced VO_2 and VCO_2 observed with GLP-1RA were normalized by treatment with both IC7Fc and GLP-1RA (Extended Data Fig. 7e–h). Movement was increased by IC7Fc and decreased by GLP-1RA (Extended Data Fig. 7i, j). Thus, IC7Fc may be advantageous as an add-on to existing incretin therapy, by preventing a loss in lean mass and minimizing the possibility of hypoglycaemic events.

IC7Fc is safe in non-human primates

For a drug to proceed into 'first in human' trials, the US Food and Drug Administration (FDA) requires that experiments be performed in two species. Non-human primates, particularly macaques that account for more than 75% of all non-human primate studies, are viewed as the closest animal model to humans. Mimicking a phase I human clinical trial, long-tail macaques (*Macaca fascicularis* 'cynomolgus') were administered a subcutaneous injection of saline (vehicle). We monitored physiological characteristics and collected blood samples at 24 h and 7 days after administration to monitor markers of inflammation and any adverse events. After 7 days of recovery, the procedure was

repeated with each macaque receiving IC7Fc (0.3 mg kg⁻¹ subcutaneously delivered) (Extended Data Fig. 8a). The macaques displayed no serious adverse events over the next 7 days and behaved normally irrespective of treatment. Here, we report a suite of markers of inflammation and blood biochemistry (Extended Data Fig. 8b–m), which demonstrate that a single IC7Fc injection is safe in non-human primates. Although these studies were encouraging, we gained further insight into whether IC7Fc may increase markers of inflammation or immunogenicity in humans by performing experiments using human peripheral blood mononuclear cells (PBMCs), obtained from 9 healthy humans and cultured for 48 h with IC7Fc (3 μ g ml⁻¹), medium alone (negative control), or mitogen phytohaemagglutinin (PHA; 5 μ g ml⁻¹; positive control to induce T cell activation and cell division). After 48 h, cell culture supernatants were collected and assayed for pro-inflammatory cytokines associated with T helper 1 (T_{H1}), T_{H2} and T_{H17} immune responses. PHA treatment increased all pro-inflammatory and T_{H1}/T_{H2}/T_{H17}-associated cytokines and reduced leptin compared with medium alone (Extended Data Fig. 8). By contrast, IC7Fc treatment was identical to that for medium alone for all measured parameters (Extended Data Fig. 8n–x), which demonstrates that IC7Fc does not activate pro-inflammatory intracellular markers or increase T_{H1}/T_{H2}/T_{H17}-associated cytokines, and has no effect on PBMC viability.

Discussion

Here we described the metabolic actions of IC7Fc that decreases hepatic steatosis and increases liver fatty acid oxidation and insulin secretion to improve glucose homeostasis. Crucially, unlike most existing drugs, IC7Fc concomitantly increases glucagon and the incretin response. This is important from a therapeutic safety point of view, as IC7Fc prevented dulaglutide (Trulicity) induced hypoglycaemic events in some mice. Furthermore, IC7Fc acutely decreases feeding, while maintaining muscle mass and preferentially decreasing fat mass, in the presence of increased energy expenditure. The ability of IC7Fc to induce muscle hypertrophy is crucially important as increased muscle mass reduces the risk of T2D¹⁸ while sarcopenia reduces mobility in the elderly²⁹. The risk of several types of fracture is increased in T2D³⁰ and some drugs that treat T2D, such as thiazolidinediones, increase skeletal fragility²¹. Here we show that IC7Fc potentially increases bone density, probably owing to its ability to increase GIP³¹, but possibly directly, as gp130

receptor ligands increase bone density³². To our knowledge, there are no current drugs that have these multiple, positive benefits to overall health and metabolism (Extended Data Fig. 9).

The clinical development of the CNTF analogue Axokine was discontinued when many treated patients developed neutralizing antibodies⁹. Unlike Axokine, IC7Fc is engineered and signals like no endogenous protein, minimizing the safety concerns of interference with endogenous protein action. In summary, we have demonstrated that the designer, chimeric gp130 receptor ligand IC7Fc decreases liver steatosis and increases insulin action, stimulating incretin secretion and circulating glucagon, which can reduce hyperglycaemia without risking hypoglycaemic events. IC7Fc also acutely decreases feeding and fat mass, while maintaining or increasing lean mass through activation of YAP1 in skeletal muscle cells. IC7Fc also increases energy expenditure, in part by activating BAT (Extended Data Fig. 9). Notably, in experiments in non-human primates, we demonstrate that IC7Fc is safe, with no signs of an inflammatory or immunogenic response. IC7Fc is, therefore, a viable and realistic biological therapy to treat T2D and muscle atrophy and we intend to progress to phase I human clinical trials.

Online content

Any methods, additional references, Nature Research reporting summaries, source data, extended data, supplementary information, acknowledgements, peer review information; details of author contributions and competing interests; and statements of data and code availability are available at <https://doi.org/10.1038/s41586-019-1601-9>.

Received: 15 May 2018; Accepted: 21 August 2019;

1. Danaei, G. et al. National, regional, and global trends in fasting plasma glucose and diabetes prevalence since 1980: systematic analysis of health examination surveys and epidemiological studies with 370 country-years and 2.7 million participants. *Lancet* **378**, 31–40 (2011).
2. Wild, S., Roglic, G., Green, A., Sicree, R. & King, H. Global prevalence of diabetes: estimates for the year 2000 and projections for 2030. *Diabetes Care* **27**, 1047–1053 (2004).
3. Carey, A. L. et al. Interleukin-6 increases insulin-stimulated glucose disposal in humans and glucose uptake and fatty acid oxidation *in vitro* via AMP-activated protein kinase. *Diabetes* **55**, 2688–2697 (2006).
4. Watt, M. J. et al. CNTF reverses obesity-induced insulin resistance by activating skeletal muscle AMPK. *Nat. Med.* **12**, 541–548 (2006).
5. Steinberg, G. R. et al. Ciliary neurotrophic factor suppresses hypothalamic AMP-kinase signaling in leptin-resistant obese mice. *Endocrinology* **147**, 3906–3914 (2006).
6. Matthews, V. B. et al. Interleukin-6-deficient mice develop hepatic inflammation and systemic insulin resistance. *Diabetologia* **53**, 2431–2441 (2010).
7. ACTS. A double-blind placebo-controlled clinical trial of subcutaneous recombinant human ciliary neurotrophic factor (rHCNTF) in amyotrophic lateral sclerosis. ALS CNTF Treatment Study Group. *Neurology* **46**, 1244–1249 (1996).
8. Duff, E. & Baile, C. A. Ciliary neurotrophic factor: a role in obesity? *Nutr. Rev.* **61**, 423–426 (2003).
9. Ettinger, M. P. et al. Recombinant variant of ciliary neurotrophic factor for weight loss in obese adults: a randomized, dose-ranging study. *J. Am. Med. Assoc.* **289**, 1826–1832 (2003).

10. Febbraio, M. A. Role of interleukins in obesity: implications for metabolic disease. *Trends Endocrinol. Metab.* **25**, 312–319 (2014).
11. Kraakman, M. J. et al. Blocking IL-6 trans-signaling prevents high-fat diet-induced adipose tissue macrophage recruitment but does not improve insulin resistance. *Cell Metab.* **21**, 403–416 (2015).
12. Rabe, B. et al. Transgenic blockade of interleukin 6 transsignaling abrogates inflammation. *Blood* **111**, 1021–1028 (2008).
13. Febbraio, M. A. gp130 receptor ligands as potential therapeutic targets for obesity. *J. Clin. Invest.* **117**, 841–849 (2007).
14. Kallen, K. J. et al. Receptor recognition sites of cytokines are organized as exchangeable modules. Transfer of the leukemia inhibitory factor receptor-binding site from ciliary neurotrophic factor to interleukin-6. *J. Biol. Chem.* **274**, 11859–11867 (1999).
15. Rakemann, T. et al. The designer cytokine hyper-interleukin-6 is a potent activator of STAT3-dependent gene transcription *in vivo* and *in vitro*. *J. Biol. Chem.* **274**, 1257–1266 (1999).
16. Harris, J. M. & Chess, R. B. Effect of pegylation on pharmaceuticals. *Nat. Rev. Drug Discov.* **2**, 214–221 (2003).
17. Jazayeri, J. A. & Carroll, G. J. Fc-based cytokines: prospects for engineering superior therapeutics. *BioDrugs* **22**, 11–26 (2008).
18. Srikanthan, P. & Karlamangla, A. S. Relative muscle mass is inversely associated with insulin resistance and prediabetes. Findings from the third National Health and Nutrition Examination Survey. *J. Clin. Endocrinol. Metab.* **96**, 2898–2903 (2011).
19. Taniguchi, K. et al. A gp130-Src-YAP module links inflammation to epithelial regeneration. *Nature* **519**, 57–62 (2015).
20. Watt, K. I. et al. The Hippo pathway effector YAP is a critical regulator of skeletal muscle fibre size. *Nat. Commun.* **6**, 6048 (2015).
21. Grey, A. Thiazolidinedione-induced skeletal fragility-mechanisms and implications. *Diabetes Obes. Metab.* **11**, 275–284 (2009).
22. Mannaerts, I. et al. The Hippo pathway effector YAP controls mouse hepatic stellate cell activation. *J. Hepatol.* **63**, 679–688 (2015).
23. Ellingsgaard, H. et al. Interleukin-6 enhances insulin secretion by increasing glucagon-like peptide-1 secretion from L cells and alpha cells. *Nat. Med.* **17**, 1481–1489 (2011).
24. Scheidt-Nave, C. et al. Serum interleukin 6 is a major predictor of bone loss in women specific to the first decade past menopause. *J. Clin. Endocrinol. Metab.* **86**, 2032–2042 (2001).
25. Whitham, M. & Febbraio, M. A. The ever-expanding myokinome: discovery challenges and therapeutic implications. *Nat. Rev. Drug Discov.* **15**, 719–729 (2016).
26. Tibble, C. A., Cavaola, T. S. & Henry, R. R. Longer acting GLP-1 receptor agonists and the potential for improved cardiovascular outcomes: a review of current literature. *Expert Rev. Endocrinol. Metab.* **8**, 247–259 (2013).
27. Glaesner, W. et al. Engineering and characterization of the long-acting glucagon-like peptide-1 analogue LY2189265, an Fc fusion protein. *Diabetes Metab. Res. Rev.* **26**, 287–296 (2010).
28. Nauck, M. et al. Efficacy and safety of dulaglutide versus sitagliptin after 52 weeks in type 2 diabetes in a randomized controlled trial (AWARD-5). *Diabetes Care* **37**, 2149–2158 (2014).
29. Larsson, L. et al. Sarcopenia: aging-related loss of muscle mass and function. *Physiol. Rev.* **99**, 427–511 (2019).
30. Ma, C., Tonks, K. T., Center, J. R., Samocha-Bonet, D. & Greenfield, J. R. Complex interplay among adiposity, insulin resistance and bone health. *Clin. Obes.* **8**, 131–139 (2018).
31. Xie, D. et al. Glucose-dependent insulinotropic peptide-overexpressing transgenic mice have increased bone mass. *Bone* **40**, 1352–1360 (2007).
32. Askmyr, M. et al. Ciliary neurotrophic factor has intrinsic and extrinsic roles in regulating B cell differentiation and bone structure. *Sci. Rep.* **5**, 15529 (2015).

Publisher's note Springer Nature remains neutral with regard to jurisdictional claims in published maps and institutional affiliations.

© The Author(s), under exclusive licence to Springer Nature Limited 2019

METHODS

Generation of IC7 and modified IC7 species. BL21-CodonPlus(DE3)-RIL cells (Agilent) transformed with pRESET5d-IC7 were grown in 400 ml Overnight Express Instant TB medium (60 g l^{-1} , Novagen) supplemented with 10 g l^{-1} glycerol and $100 \mu\text{g ml}^{-1}$ ampicillin for 2 h at 37°C then a further 62 h at 22°C . IC7 was purified from inclusion bodies by solubilization with 6 M guanidine hydrochloride and refolded using dialysis. The soluble protein was then purified by ion exchange chromatography on HiTrap Q HP columns (GE Healthcare), desalted and reacted with methoxy PEG propionaldehyde (30 kDa and 40 kDa; JenKem Technology) in the presence of sodium cyanoborohydride. The PEGylated IC7 was separated from the unreacted PEG by anion exchange chromatography and mono-PEGylated IC7 was isolated by gel filtration in PBS (Superdex 200 26/60 GE Healthcare). A synthetic DNA sequence encoding a sequence-optimized IC7Fc coding region incorporating a short spacer sequence between the IC7 coding region and the human IgG1 hinge region, together with L234A/L235A mutation, was synthesized by GeneArt and sub-cloned into pEE14.4 (Lonza) in the Fc region, which prevents binding to the Fc receptor in a manner similar to Enbrel³⁵. Transfection of suspension-adapted CHOK1SV cells (RRID:CVCL_DR95, Lonza, supplied under a research-only licensing agreement) was performed using FuGENE (Promega) with cells (1×10^6) in CD CHO medium (Thermo Fisher Scientific) plated in six-well plates. Twenty-four hours after transfection, cells were expanded across 96-well plates and selection initiated with $50 \mu\text{M}$ methionine sulfoximine. Stable transfectants were screened for IC7Fc secretion, positive cultures expanded and the highest producing line selected for scale-up culture. Recombinant IC7Fc was purified by affinity (Protein A-Sepharose; GE Healthcare) and size exclusion (Superdex 200; GE Healthcare) chromatography under low endotoxin conditions (<0.5 endotoxin units per mg).

IL-6/gp130 receptor binding assay. Human IL-6 (CYT-213, ProSpec-Tany TechnoGene) was labelled with europium using the DELFIA kit (1244-302, Perkin Elmer) as per manufacturer's instructions. The IC7 binding assays were performed by coating wells of a 96-well Lumitrac plate with $0.1 \mu\text{g sgp130Fc}$ (671-GP, R&D systems) in PBS (pH 7.4) for 90 min at room temperature. Wells were blocked with $50 \mu\text{l}$ 0.5% ovalbumin in TBS for 60 min at 37°C before being washed with TBST (pH 7.0) four times. Decreasing concentrations of unlabelled IC7/modified IC7 were incubated with $0.2 \mu\text{g}$ per well sIL-6R (227-SR/CF, R&D Systems) and europium-labelled IL-6 in assay buffer (1244-111, Perkin Elmer) for 90 min at room temperature. The plate was washed 6 times with TBST before incubating with $50 \mu\text{l}$ enhancement solution (4001-0010, Perkin Elmer) for 15 min at room temperature. Europium counts were read on a Wallac Victor2 1420 Multilabel Counter capable of TRF (excitation 340 nm /emission 615 nm).

Haptoglobin secretion assay. HepG2 cells were grown in growth medium (DMEM low glucose, 10% FBS, 1% penicillin/streptomycin), seeded in 96-wells until confluent before being serum-deprived for 60 min before treated with unlabelled IC7/modified IC7 or vehicle in triplicate for 24 h in serum-free medium. Supernatant was collected and haptoglobin quantified by using a haptoglobin enzyme-linked immunosorbent assay (ELISA) kit (US Biological H1820-04) as per manufacturer's instructions.

IC7 signalling and expression. HepG2 cells were grown as per haptoglobin assays, serum deprived for 12 h before being treated with described amounts of unlabelled IC7/modified IC7 and vehicle (saline). Mouse tissues were generated as per the 'Acute mouse studies' section. Tissues were lysed, and the protein concentration was determined BCA protein assay kit (Life Technologies). Lysates were solubilized, $40 \mu\text{g}$ protein was loaded and resolved by SDS-PAGE on polyacrylamide gels, transferred to membranes, and blocked with 5% milk or bovine serum albumin (BSA). Immunoblotting was performed using the following primary antibodies pSTAT3 (Tyr705) Ab (9131, Cell Signaling) or pSTAT3 (Y705) (9145 Cell Signaling, Clone D3A7), total STAT3 antibody (9139, Cell Signaling, clone 124H6) or STAT3 (06-596, Upstate, Millipore), GAPDH (2118, Cell Signaling, clone 14C10), β -actin (4967, Cell Signaling). After incubation with appropriate secondary antibody, the immunoreactive proteins were detected with enhanced chemiluminescence.

Activation of Hippo pathway. Western blots and qPCR assays were performed on samples provided from the Pair Feeding Study. All reagents were purchased from Sigma-Aldrich unless stated.

Protein extraction and western blotting. Mouse gastrocnemius skeletal muscle was lysed in homogenization buffer (protein concentrations were determined using the bicinchoninic acid (BCA) assay as per manufacturer's instructions (Thermo Fisher Scientific). Proteins were separated and transferred to PVDF-FL membranes (Bio-Rad Laboratories) that were air-dried at room temperature for 15 min before re-hydration in absolute methanol and blocking for 60 min at room temperature in 5% non-fat milk that was diluted in PBS. Membranes were incubated overnight with primary antibodies, followed by incubation for 60 min at room temperature with horseradish peroxidase (HRP)-conjugated secondary antibodies and detection using ECL detection reagent (GE Healthcare Life Sciences). Primary antibodies used were total YAP1 (14074), phosphorylated YAP1(Ser127) (4911),

both 1:1,000 dilution from Cell Signaling Technologies. Secondary antibody was goat anti-rabbit (1706516, Bio-Rad technologies, 1:5,000 dilution). Densitometry was performed using ImageJ software (version 1.52f with Java 1.8.0_172 (64bit) (<http://rsb.info.nih.gov/ij/index.html>). Total protein levels as assessed by PonceauS staining of the membrane after transfer were used for normalization.

Quantitative reverse transcriptase PCR. Total RNA was extracted from 10–20 mg of gastrocnemius muscle using TRIzol (Life Technologies) as per the manufacturer's protocols. Reverse transcription was performed using Multiscribe reverse transcriptase (Life Technologies) as per manufacturer's protocols on $1 \mu\text{g}$ of total RNA. Transcripts were measured using Taqman fluorogenic primer probe sets (Life Technologies). Primers used were *Yap1* (Mm01143263_m1), *Ankral1* (Mm00496512_m1) and *Cyr61* (Mm00487499_g1) with the levels of mouse *18S* (also known as *Rn18s*) (4319413E) used to normalize samples for analysis by the $\Delta\Delta C_t$ method³⁴.

C2C12 cell culture and siRNA transfection. C2C12 myoblasts were cultured in growth medium (DMEM (11965-092; Life Technologies) containing 10% HyClone fetal bovine serum (FBS) (SH30071.03; GE Healthcare Life Sciences) at 37°C and 95% O_2 /5% CO_2 and maintained at a density below 70% confluence. Cells were seeded into black walled 96-well plates (3340; Corning) containing 40 nM ON-TARGETplus non-targeting pool negative control siRNA (OTP; D-001810-10) or ON-TARGETplus siRNA SMARTpool targeting mouse *Yap1* (siYAP; L-046247-01-0005; Dharmacon) (see Supplementary Note S5 for siRNA sequences), $0.2 \mu\text{l}$ of Dharmafect 4 transfection lipid reagent (T-2004-1; Dharmacon) and $15.8 \mu\text{l}$ of OptiMEM-1 reagent (31985-062; Life Technologies) at a density of 5,000 cells per well. After 24 h, medium was replaced. After a further 24 h, when cells were confluent, growth medium was replaced with differentiation medium (DMEM containing 2% horse serum (16050-122; Gibco). Differentiation medium was replenished every 48 h for a total of 96 h. After this time, cells were placed in DMEM containing 10 mM glucose and 10% FBS in the presence of vehicle control (PBS) or IC7Fc (1 ng ml^{-1}) for a further 24 h. Cells were either lysed for protein extraction and western blotting or fixed in 4% paraformaldehyde in PBS for 10 min at room temperature for immunolabelling and determination of myofibre width.

C2C12 immunolabelling and determination of myofibre width. C2C12 myotubes were fixed in 4% paraformaldehyde in PBS for 10 min at room temperature, washed once in PBS then permeabilized in PBS containing Triton X-100 (0.1%; PBS-T) for 10 min at room temperature. Cells were incubated in blocking buffer (1% BSA in PBS-T) for 2 h at room temperature, then incubated in blocking buffer containing primary antibody against sarcomeric myosin (MF-20; Developmental Studies Hybridoma Bank; 1:50 dilution) at 4°C on a rocker with gentle agitation overnight. The next day, cells were washed three times with PBS and then incubated in blocking buffer containing secondary antibody (Alexa Fluor 555 conjugated goat anti-mouse IgG2b (A21147; Life Technologies; 1:500 dilution) for 2 h at room temperature on a rocker with gentle agitation in the dark. Cells were washed 3 times in PBS and imaged in a 96-well plate on a Zeiss Axiovert 40 CFL microscope. Average myofibre width was determined by measuring fibre width 5–10 times randomly along the length of a myofibre. At least 6 myofibres were measured per field of view in a total of 3–4 independent fields of view per condition. For the quantification, three random fields of view per well were taken at the same magnification.

qPCR mouse liver. Total RNA was isolated from liver with Tri Reagent (Sigma-Aldrich) and reverse transcribed to cDNA with the use of random hexamers. Quantitative PCR (qPCR) was performed on a 7500 Fast Sequence detector (Applied Biosystems). Each assay included a no-template control and a no-reverse transcriptase control. The relative concentrations of measured mRNA were determined by plotting the threshold cycle versus the log of the serial dilution points, and the relative expression of *SREBP1c* (Mm01197412_g1) and *Dgat1* (Mm01197412_g1) was determined after normalization to the housekeeper gene *18S* (Hs99999901_s1).

AMPK activity assay in mouse liver. AMPK activity assays were conducted as previously described³⁵. In short, liver tissues were homogenized in buffer (50 mM Tris pH 7.5, 1 mM EDTA, 10% glycerol, 1% Triton X-100 with 1 mM dithiothreitol (DTT), 1 mM PMSF, $5 \mu\text{l ml}^{-1}$ protease inhibitor cocktail, $10 \mu\text{g ml}^{-1}$ trypsin inhibitor, 50 mM NaF, 5 mM Na pyrophosphate). Liver homogenates were incubated with AMPK α 1 or AMPK α 2 antibody-bound protein A beads for 2 h at 4°C . Complexes were washed 3 times before being suspended in 0.05 M Tris pH 7.5. AMPK activity was then assessed in the complexes and calculated as counts per minute of phosphate (from $[\gamma\text{-}^{32}\text{P}]\text{ATP}$) incorporated into the SAMS peptide ($\text{ACC}\alpha(73\text{--}87)\text{A}^{77}$) per minute per milligram total protein in the immunoprecipitate.

Human PBMC immunoassay. The human PBMC samples were obtained from buffy coats supplied by the Australian Red Cross Blood Service under agreement. In the written and signed agreement, the stated purpose was to use the human PBMCs as controls from immunological assays. Nine different donor samples were used, with one being tested twice as an internal control. Human PBMC samples

were cultured for 48 h (37°C; 5% CO₂) in the presence of IC7Fc (3 µg ml⁻¹) with and without Fc-block (BD, 564220); medium alone (negative control); or with the mitogen PHA (5 µg ml⁻¹) as a positive control to induce T cell activation and cell division. The duration of culture was for 48 h to allow detection of cell activation and proliferation following PHA stimulation, and to provide sufficient time in culture for IC7Fc to induce detectable effects. Cell culture supernatants were collected, stored at -80°C and later analysed in a single assay for proinflammatory and T_H1/T_H2/T_H17 associated cytokines by the multiplex method. PBMCs were collected (immediately after collecting supernatant samples) and analysed for expression of cell surface and intracellular markers by flow cytometry.

Human PBMC multiplex assay. Milliplex Human Adipokine 9-plex panel (HADK2MAG-61K) and Bio-Rad Human Cytokine Group 1 3-plex panel (Z5000006ZE) were used as per manufacturer's instructions. The multiplex analysis was performed on a Bio-Plex 200 Reader and analysed using Bio-Plex Manager 5.0 and Excel version 15. Duplicate aliquots were tested where sufficient sample volume was available (all 9-plex assay, selected 3-plex tests).

Mouse islet isolation and GSIS. Islets were isolated from 10-week-old male C57BL/6 mice. After pancreatic digestion, islets were purified using a Ficoll gradient and centrifugation. Batches of five islets were picked, with at least six replicates per group, and insulin secretion assays carried out, as follows: islets were preincubated for 60 min in Krebs's Ringer HEPES buffer (KRHB) containing 0.1% BSA and 2.8 mM glucose. Then, islets were incubated for 60 min at 37°C with KRHB (plus 0.1% BSA) containing 2.8, 8.3 or 20 mM glucose. An aliquot of the buffer was taken, and insulin release measured using RIA. Stimulation of isolated pancreatic islets from untreated mice was performed in the presence of 30 or 100 ng ml⁻¹ IC7Fc. For acute inhibitor studies, islets from chronically treated HFD mice were isolated, IC7Fc or Ex(9-39) were present at 100 ng ml⁻¹ or 100 nM, respectively during the 60 min glucose stimulation only. An aliquot of the buffer was taken, and insulin release measured using the homogenous time-resolved fluorescence assay (HTRF, Cisbio). Subsequently secretion in supernatant and content in neat islet lysates were analysed with hormone kits described above. Active GLP-1 levels were quantitated using commercially available ELISA kits, according to manufacturer's instructions (EGLP-35K, Merck Millipore).

Human tissue collection for ex vivo studies in human colonic mucosae. Patients gave written informed consent for colon tissue donation from resected large intestine at Flinders Medical Centre and Flinders Private Hospital approved by the Southern Adelaide Clinical Human Research Ethics Committee. Human colonic tissue was obtained from patients undergoing bowel resection for cancer (Supplementary Table 1). Samples were obtained from sites at least 10 cm distal from the tumour location. Specimens from patients that were indicated for any form of inflammatory bowel disease were excluded from this study. Characteristics of the patient cohort are listed in Supplementary Table 2. None of the patients had diabetes. The specimens were immediately placed in iced-cold Krebs buffer (138 mM NaCl, 4.5 mM KCl, 2.6 mM CaCl₂, 4.2 mM NaHCO₃, 1.2 mM MgCl₂, 1.2 mM NaH₂PO₄, 10 mM HEPES and 5 mM glucose) and transported to the laboratory for dissection within 15 min. The specimens were rinsed with iced-cold Krebs buffer to remove any luminal content and dissected clear of adipose, muscular and connective tissue. The mucosae were gently dissected off from the submucosae as intact sheets using a stainless steel spatula, cut into 5 mm pieces and weighed individually. The mucosal pieces were then transferred to a 96-well plate for secretion assays.

Secretion experiments. Mucosal pieces were incubated with 200 µl of buffer (control) or buffer containing various concentrations of IC7 (from 1 ng ml⁻¹ up to 1 µg ml⁻¹) or positive controls (described in detail below) in a 96-well plate for 15 min. The buffer was a modified Krebs buffer with the addition of 1 µM sitagliptin, 0.1% fatty-acid-free BSA (A1595, Sigma Aldrich) at pH 7.4. After incubation at 37°C in 95% O₂/5% CO₂, supernatants were collected and stored in aliquots at -20°C. Active GLP-1 levels were quantitated using commercially available ELISA kits, according to manufacturer's instructions (EGLP-35K, Merck Millipore). IBMX and FSK (I5879 and F6886, respectively, Sigma Aldrich; 10 µM each) and 70 mM KCl were used as positive controls. For the 70 mM KCl solution, an equimolar amount of NaCl was removed to maintain osmolarity. Only samples that show positive response to at least one positive control (70 mM KCl or 10 µM IBMX and FSK) were included in analysis.

Mouse experiments. Unless otherwise stated, all mouse experiments used male, C57BL/6j mice, bred and housed at the Alfred Medical Research and Education Precinct Animal Centre (AMREP PAC) or the Garvan Institute in a pathogen-free facility under controlled environmental conditions and exposed to a 12:12 h light:dark cycle. Mouse experiments were approved by the Alfred Medical Research and Education Precinct Animal Ethics Committee or the Garvan Institute/St Vincent's Hospital Animal Ethics Committee and conducted in accordance with the National Health and Medical Research Council (NHMRC) of Australia Guidelines for Animal Experimentation. All experiments commenced when mice were 6–8 weeks of age. Mice were fed either a chow diet (5% of total energy from fat) or a HFD (43% of total energy from fat) (Speciality Feeds) for

4–10 weeks depending on the experiment. Mice were given their prescribed diet and water ad libitum except where other specified. Tissues were collected and snap frozen in liquid nitrogen before storage at -80°C. Blood from anaesthetized mice (4% isoflourane at euthanization) was collected by cardiac puncture and blood from live mice was collected from a tail snip. Blood was collected in EDTA-coated tubes containing inhibitors (aprotinin for glucagon, DPP-IV inhibitor for active GIP and GLP-1). After centrifugation, plasma was aliquoted and stored at -80°C. Plasma insulin levels were measured using Mouse Ultrasensitive Insulin ELISA kit (80-INSMSU-E01) as per manufacturer's instructions. Plasma C-peptide was measured using the Crystal Chem (90050) Mouse C-peptide ELISA kit as per manufacturer's instruction. Plasma glucagon levels were measured using the Glucagon ELISA kit (81518, Crystal Chem). Plasma total and active GIP were measured using ELISA kits (81511 and 81517, respectively; Crystal Chem). GLP-1 measurements were performed using a High-Sensitive ELISA kit (EZGLPHS-35K, EMD Millipore). Plasma NEFA levels were measured using Wako NEFA assay kits (999-34691 and 993-35191). All assays were performed according to the manufacturers' instructions. For OGTTs, mice were fasted for 5–6 h and challenged with glucose by oral gavage (2 g glucose per kg lean body mass). Blood was collected by tail nipping at -30, 0, 15, 30, 45, 60, 90 and 120 min after glucose challenge. Body composition (lean and fat mass) was measured using an EchoMRI. Blood glucose was measured using an Accu-chek glucometer and glucose strips. For metabolic caging experiments, mice were acclimatized for 2 days before indirect calorimetry started (Columbus Instruments). See Supplementary Note S3 for calculations.

Pharmacokinetic assay. Chow-fed mice were injected intraperitoneally with the indicated dose of IC7 or IC7Fc. Plasma samples were taken at given time points, spun at 5,000 r.p.m. for 10 min before being frozen for later analysis.

Single-dose pharmacokinetics. Two cohorts of 5 mice were intraperitoneally treated with IC7 (1 mg kg⁻¹) with blood samples taken at 0, 30 min, 1 h, 2 h (cohort 1) and 0, 30 min, 1 h, 6 h (cohort 2). Five cohorts of 5 mice were intraperitoneally treated with IC7Fc (1 mg kg⁻¹) and blood samples taken at 0, 30 min, 1 h, 2 h (cohort 1), 0, 1 h, 2 h, 6 h (cohort 2), 0, 2 h, 6 h, 12 h, 24 h (cohort 3), 0, 2 h, 24 h, 36 h, 48 h (cohort 4), 0, 2 h, 12 h, 36 h, 48 h, 72 h (cohort 5).

Cytokine ELISAs. IC7 and IC7Fc were quantified using a custom ELISA kit. High protein binding ELISA plates were coated with 2 µg ml⁻¹ anti-IL-6 capture antibody (eBioscience, 14-7069) overnight at 4°C. Wells were blocked with diluent (PBS, pH 7.4, with 1% ELISA grade BSA) for 2 h at 37°C. Wells were washed 6 times with wash buffer (PBS pH 7.4, 0.05% Tween-20) before incubation with samples and standards in diluent for 90 min. IC7 and IC7Fc served as the standards for their respective samples. Wells were washed 6 times with wash buffer before incubation with 0.5 µg ml⁻¹ human IL-6 secondary antibody (R&D Systems, AB-206-NA) for 90 min. Wells were washed four times with wash buffer and with detection antibody (Santa Cruz, 2020) incubated for 60 min. 3,3',5,5'-Tetramethylbenzidine (TMB) was added for 5–15 min before stopping with 1 M HCl and plates were read at 450 and 540 nm.

Chronic mouse studies. Mice were fed a HFD for 8 weeks before being treated daily for 7 days with vehicle (saline), IC7Fc (1 mg kg⁻¹), mIC7A (1 mg kg⁻¹) or mIC7B (1 mg kg⁻¹), then fasted, anaesthetized with 50 mg kg⁻¹ pentobarbital (Sigma) and killed on day 8. On day 4, mice were fasted overnight and then given an intraperitoneal glucose tolerance test (2 g per kg per lean mass glucose). Liver palmitate oxidation was measured as previously described³⁶. Next, mice were fed a HFD for 8 weeks before being treated every second day for 15 days (eight injections in total) with vehicle (saline) or IC7Fc (1 mg kg⁻¹). Body weight was measured on days 1, 2, 3, 5, 7, 9, 13 and 16. Body composition was measured on days 1, 5, 11 and 16. Mice were placed in the Comprehensive Laboratory Animal Monitoring System (Oxymax/CLAMS, Columbus Instruments) at 30°C immediately on day 13, injected intraperitoneally late afternoon before being left for another 48 h, and removed on day 15. Mice were fasted (4 h), anaesthetized with pentobarbital (Sigma) 50 mg kg⁻¹ and killed on day 16.

Seven-day paired-feeding experiment. Mice were fed a HFD for 8 weeks before being treated daily for 7 days with vehicle (saline) or IC7Fc (1 mg kg⁻¹). Vehicle pair-fed mice commenced 1 day after the IC7Fc-treated and ad libitum vehicle-treated mice to ensure accurate pair feeding. Food intake was measured daily. Mice were fasted for 4 h before an OGTT (2 g per kg lean body mass) on day 5. Mice were fasted (4 h) anaesthetized with 50 mg kg⁻¹ pentobarbital (Sigma) and killed on day 8.

Lipidomics. Triacylglycerol and diacylglycerol levels were measured as previously described with minor modifications³⁷. In brief, liver samples were homogenized and sonicated in PBS (pH 7.4), a protein assay was conducted, and 25 µg of each sample aliquoted and used for lipid extraction. An internal standard mixture (ISTD) and CHCl₃:methanol (2:1) were added to the samples before being vortexed, mixed, sonicated and centrifuged. The supernatant containing the lipid was removed and dried, before the lipids were resuspended in H₂O-saturated butanol then sonicated, before methanol with 10 mM ammonium was added. The resuspended samples were centrifuged and the supernatant transferred to

glass vials. Lipidomic determination was performed on the samples by liquid chromatography–electrospray ionization–tandem mass spectrometry (LC–ESI–MS) combined with triple quadrupole mass spectrometer. Data were analysed using MultiQuant software v.1.2 and normalized to the total phosphatidylcholine levels of each sample.

STZ treatment. Six-week-old chow-fed mice were fasted for 4 h then injected with STZ (Sigma–Aldrich) (55 mg kg⁻¹ in 0.1 M citrate buffer, pH 4.5) every day for 5 days and left to recover for 4 weeks. Blood glucose was monitored and all mice with a fasting blood glucose over 16 mM were considered diabetic. Mice were fasted for 4 h then intraperitoneally injected with IC7Fc. Blood glucose was monitored over 24 h before being fasted for 4 h and injected with IC7Fc again and monitored for a further 24 h. The upper limit of the blood glucose monitor was 33.3 mM. Where levels exceeded this, blood samples were diluted in gelofusine and blood glucose measured again. Mice were fasted for 6 h then killed and tissues and plasma taken.

Acute mouse studies. Mice were fed a chow or HFD for 4 weeks before intraperitoneal injection in the fed state with vehicle (saline) or IC7Fc 1 mg kg⁻¹. Glycaemia was monitored taking blood glucose repeatedly over 6 h. Two days later, they were injected with identical treatments again, anaesthetized with 50 mg kg⁻¹ pentobarbital (Sigma) in plasma, and snap-frozen tissues samples were taken 30 min and 2 h after injection. Alternatively, mice were fed a chow or a HFD for 4 weeks before being fasted and injected intraperitoneally with vehicle (saline) or 1 mg kg⁻¹ IC7Fc 30 min before an OGTT (as outlined earlier).

Escalating dose blood glucose. There were ten cohorts of mice, five cohorts receiving intraperitoneal injections and five cohorts receiving subcutaneous injection. Within each of these cohorts, there were five groups of five mice. Mice were injected with a low dose of IC7Fc (0.1 mg ml⁻¹) and blood glucose measurements were taken at 0, 1 h, 2 h (group 1), 0, 4 h, 8 h (group 2), 0, 12 h, 24 h (group 3), 0, 30 h, 36 h (group 4), 0, 36 h, 48 h (group 5). Another groups of five mice received vehicle. After a 2-week wash-out period, the experiment was repeated at a high dose of IC7Fc (1 mg kg⁻¹).

db/db study. Seven-week-old male mice from the strain BKS.Cg-*Dock7*^{tm+/+}/*Lepr*^{db/db} (strain 000642) were purchased from Jackson Laboratory. The experimental procedures performed were approved by the Garvan Institute/St Vincent's Hospital Animal Ethics Committee and were in accordance with the National Health and Medical Research Council of Australia's guidelines on animal experimentation. Two genotypes were studied: homozygous (*Lepr*^{db/db}) and lean heterozygous within-colony controls (*Dock7*^{tm+/+}/*Lepr*^{db}). Mice were randomly allocated to experimental groups (two genotypes and two treatment groups). They received a single intraperitoneal dose of vehicle (saline) or IC7Fc (1 mg kg⁻¹) in the fed state at 7, 13 and 17 weeks of age and blood glucose was monitored over 6 h. Body weight was recorded every second day and body composition (fat and lean mass) was determined weekly. Fasting blood glucose and insulin levels were measured 17 days after the first intraperitoneal injection (approximately 10-week-old mice).

Stable isotope experiment. Mice were fed a HFD for 4 weeks before being fasted for 4 h and gavaged (2 g per kg lean body mass) with pure D-[6,6'-²H₂]glucose (Cambridge Isotope Laboratories) as previously described³⁸. Blood glucose was measured 30 min before and at 15, 30, 60 and 120 min after gavage, with blood (about 10 µl) also collected for tracer enrichment analysis at these time points. Blood was centrifuged (4 °C, 8,000 r.p.m.) and plasma used for analysis of isotope enrichment via gas chromatography–mass spectrometry (GC–MS).

IC7 euglycaemic experiments: surgery procedure. Mice were anaesthetized with isoflurane (4% induction, 1.5–2% maintenance) for insertion of catheters into the left carotid artery and right jugular vein as previously described³⁹. In brief, free catheter ends were tunnelled under the skin, externalized at the neck and sealed. Mice were then singly housed and monitored daily. Catheters were flushed every 1–2 days with heparinized saline to maintain patency. Five to seven days after surgery, mice were randomly divided into treatment groups. IC7Fc euglycaemic clamp studies were performed in mice after a 6-h overnight fast. Mice were conscious, unrestrained and were not handled during the procedure to minimize stress. At 90 min before infusion (–90 min), a primed (5 µCi), continuous infusion (0.05 µCi min⁻¹) of [3-³H]glucose (PerkinElmer) was commenced. At –30, –20, –10 and 0 min, samples were collected for basal glucose turnover (Rd) and glucose levels. At time 0, an intravenous bolus injection of IC7Fc (1 mg kg⁻¹) was administered. To maintain glycaemia at basal levels, blood samples were taken every 15 min and glucose (25% w/v) was infused as necessary. Red blood cells from each sample were resuspended in heparinized saline and returned to the mouse. In addition, two sequential samples were taken for glucose turnover at 60, 120 and 180 min after IC7Fc bolus injection. For all experiments in which octreotide (Abcam) was applied, octreotide was dissolved in sterile water and stocks were stored frozen in 1 mg ml⁻¹ concentrations (see Supplementary Note S1). On the day of experiment, the stock solutions were diluted with gelofusine to the final concentration. Octreotide infusion (7.5 µg kg⁻¹ min⁻¹) commenced 30 min before bolus injection of IC7Fc. For estimation of glucose uptake into tissues, a bolus injection of [¹⁴C] 2-deoxyglucose (13 µCi; PerkinElmer) was administered as an intravenous bolus

injection 180 min after IC7Fc bolus injection, and blood was sampled at 1, 2, 5, 10, 20, 30 and 40 min. Mice were then euthanized and organs were removed, snap frozen in liquid nitrogen, and stored at –80 °C for further analysis. For calculations, see Supplementary Note S2.

Incretin receptor knockout experiments. Whole-body DIRKO mice were generated as previously described⁴⁰. Mice from the same litter or family were studied and housed under specific-pathogen-free conditions in microisolator cages, maintained on a 12 h light/dark cycle with free access to standard rodent diet and water, unless noted otherwise. All experiments were carried out in accordance with protocols and guidelines approved by the Animal Care Committee at Mt. Sinai Hospital and the Toronto Centre for Phenogenomics. Starting at 6 weeks of age, male mice were placed on a 45% fat diet (Research Diets, D12451) for 4 weeks before undergoing an OGTT. For OGTTs, mice were fasted for 5 h and then given a single intraperitoneal injection of vehicle (saline) or 1 mg kg⁻¹ IC7Fc 30 min before receiving oral glucose (2 g per kg lean body mass) by gavage. Blood glucose levels were measured in tail-vein blood samples just before IC7Fc administration and for up to 120 min after oral glucose administration.

GLP-1RA study. Mice were fed a HFD, then subjected to metabolic cage studies and fed the diet for another 3–4 weeks. After 7–8 weeks, DIO mice received a subcutaneous injection of saline (vehicle) IC7Fc (0.5 mg kg⁻¹), dulaglutide (GLP-1RA; 0.5 mg kg⁻¹) or a combination of the latter (IC7Fc + GLP-1RA) in the fed state, and glycaemia was monitored over the duration of 6 h with terminal cardiac puncture to obtain plasma sample for hormone measurements. For metabolic caging experiments, 4-week-old DIO mice were acclimatized for 2 days before receiving a single subcutaneous injection at 19:00 and indirect calorimetry was started (Oxymax/CLAMS, Columbus Instruments).

Generation of ROSA26-IC7Fc mice. cDNA of IC7Fc was amplified via PCR from a plasmid with codon-optimised IC7Fc sequence using primers 5'-AAAG GCGCGCCACCATGAACAGCTTCTCCAC-3' and 5'-AAAGGCGCGCCTCA TTTGCCGGGGCTCAGGGA-3' and cloned into the AscI site of the STOP-eGFP-ROSA-CAG targeting vector⁴¹. Approximately 1 × 10⁷ Bruce4 ES cells were transfected with the ROSA26-IC7Fc targeting vector and successful integration of the construct into the ROSA26 locus was verified by Southern blot analysis. Successfully targeted embryonic stem cell clones were injected into blastocysts. Resulting chimeric mice were backcrossed to C57BL/6 mice and germline transmission was verified by genomic PCR analysis using primers 5'-TGTCGCAAATTAAGTGTGAATC-3', 5'-GATATGA AGTACTGGGCTCTT-3', and 5'-AAAGTGCCTCTGAGTTGTTATC-3'. To generate mice that express IC7Fc from liver tissue, we crossed litters of ROSA26-IC7Fc mice with Alb-Cre-expressing mice to yield IC7Fc^{Alb-cre} mice. *Alb-cre*^{+/+} (B6.Cg-Tg(Alb-cre)21Mgn/J) mice were obtained from the Jackson Laboratory. ROSA26-IC7Fc mice were bred to *Alb-cre* mice to generate IC7Fc^{+/+} *Alb-cre*^{-/-} (IC7Fc^{Alb-cre}) mice. To generate mice expressing IC7Fc from muscle, we crossed litters of ROSA26-IC7Fc mice with MCK-Cre-expressing mice to yield IC7Fc^{MCK-cre} mice. *MCK-cre*^{+/+} mice were obtained from Jackson Laboratory.

Phenotyping of IC7Fc^{Alb-cre} and IC7Fc^{MCK-cre} mice. An initial group of IC7Fc^{Alb-cre} and IC7Fc^{WT} mice we placed on a standard chow diet and killed after 8 weeks for the measurement of plasma IC7 and pSTAT3 in tissues. A separate cohort of mice was fed a chow diet or a HFD from 10 weeks of age for a further 6 weeks before being killed. A third group of IC7Fc^{Alb-cre} and IC7Fc^{WT} mice were fed a standard chow diet and monitored from 6 weeks until 19 weeks of age before being killed and blood hormones were measured. IC7Fc^{MCK-cre} and IC7Fc^{WT} mice were maintained at thermoneutrality (30 °C) from 7 to 8 weeks of age and fed a HFD for a further 6 weeks before being killed and blood hormones and metabolites measured and for muscle weight measures. A second cohort of female IC7Fc^{MCK-cre} and IC7Fc^{WT} mice were maintained at 22 °C on a standard chow diet from 6 until 26 weeks for bone scans.

Micro-computed tomography. Bone samples from female IC7Fc^{Alb-cre} and floxed control mice were analysed using a Skyscan Model 1172 MicroCT scanner (Bruker) at 50 kV, 200 mA with a 0.5-mm aluminium filter using a pixel size of 4.3 µm. Scanned images were captured every 0.4° to 180°, reconstructed and analysed by NRecon software (v.1.6.10.5). A standard trabecular region of interest 1 mm in length was chosen starting 0.5 mm from the distal femoral growth plate, excluding cortical bone. CTAnalyser software (v.1.16.1.0) was applied to quantify cancellous bone volume and microarchitecture, using global threshold values of 85–255.

Non-human primate studies. Non-human primate experiments were approved by the Monash University Animal Ethics Committee and conducted in accordance with the National Health and Medical Research Council (NHMRC) of Australia Guidelines for Animal Experimentation. Characteristics of monkeys can be found in Supplementary Table 3. Three male, long-tail 'cynomolgus' macaques (Supplementary Table 2) were fasted overnight before being restrained in crush mechanism and sedated with acetyl promazine and diazepam. Anaesthesia was induced using 6–8% sevoflurane in 100% oxygen. Once anaesthetized, an appropriately sized endotracheal tube was placed into the windpipe with its cuff

inflated. Macaques were maintained in an anaesthetized state with a gas anaesthetic machine using sevoflurane 1–3% and 100% oxygen. Macaques received ongoing monitoring of anaesthetic depth and physiological parameters by observation and pulse oximetry. Eyes were lubricated to prevent drying. The macaques' body temperature was maintained by a hot air cocoon, plus a warm air circuit on the anaesthetic machine. Basal blood samples were taken by the saphenous vein before subcutaneous injection with vehicle (saline) or IC7Fc (0.3 mg kg⁻¹). Blood samples were taken at 20, 60 and 90 min. Once all biological samples were collected, the anaesthetic sevoflurane was turned off and the macaques were maintained on 100% oxygen for a 2–5 min. Once heart rate and respiratory rate started to rise, the endotracheal tube was removed and the macaque was returned to the primate housing unit, placed in the recovery position and observed for rate and character of breathing, return of consciousness and righting reflex. Macaques have to be returned promptly to the primate housing unit so they can regain consciousness very quickly. Blood samples were also taken at 24 h and 7 days after injection. All macaques were treated with vehicle first, allowed to recover for a week after the 7 day blood sample before being treated with IC7Fc. Blood samples were sent to a commercial pathology service for analysis.

Statistics. No statistical methods were used to predetermine sample size. The investigators were not blinded to allocation during experiments and outcome assessment. Data were analysed by several appropriate statistical tests. Samples had to pass the D'Agostino and Pearson normality test before statistical analysis using a parametric test. If the sample size was too small (<8 per group) the Shapiro–Wilk normality test was applied. If both normality tests failed, a non-parametric test was applied. The statistical differences between groups were determined using the following parametric tests: when two measures were compared (for example, fasting glucose IC7Fc versus vehicle), data were analysed by unpaired two-tailed Student's *t*-test. When several measures at one time point were compared (for example, fasting glucose (vehicle ad libitum, vehicle pair-feeding, and IC7Fc ad libitum), data were analysed using a one-way ANOVA with Tukey's multiple comparisons test. When two or more conditions with several time points were compared (for example, blood glucose in vehicle- or IC7Fc-treated mice over time), data were analysed using a two-way (condition by time) repeated-measures ANOVA with either Sidak's or Tukey's multiple comparison test as appropriate. The two-tailed unpaired Mann–Whitney *U*-test was applied as a non-parametric test for the comparison of two measures. When several measures needed to be compared, the nonparametric Kruskal–Wallis test and Dunn's multiple comparisons test were applied. The GraphPad Prism 7/8 statistical software package was used to compute these statistics. See Supplementary Note S4 for further details.

Reporting summary. Further information on research design is available in the Nature Research Reporting Summary linked to this article.

Data availability

All raw data for all figures are available at https://monash.figshare.com/articles/Treatment_of_type_2_diabetes_with_the_designer_cytokine_IC7Fc/9637040.

33. Hezareh, M., Hessel, A. J., Jensen, R. C., van de Winkel, J. G. & Parren, P. W. Effector function activities of a panel of mutants of a broadly neutralizing antibody against human immunodeficiency virus type 1. *J. Virol.* **75**, 12161–12168 (2001).
34. Schmittgen, T. D. & Livak, K. J. Analyzing real-time PCR data by the comparative C_T method. *Nat. Protocols* **3**, 1101–1108 (2008).
35. Chen, Z. P. et al. Effect of exercise intensity on skeletal muscle AMPK signaling in humans. *Diabetes* **52**, 2205–2212 (2003).
36. Henstridge, D. C. et al. Genetic manipulation of cardiac Hsp72 levels does not alter substrate metabolism but reveals insights into high-fat feeding-induced cardiac insulin resistance. *Cell Stress Chaperones* **20**, 461–472 (2015).

37. Jordy, A. B. et al. Analysis of the liver lipidome reveals insights into the protective effect of exercise on high-fat diet-induced hepatosteatosis in mice. *Am. J. Physiol. Endocrinol. Metab.* **308**, E778–E791 (2015).
38. Kowalski, G. M. et al. Overexpression of sphingosine kinase 1 in liver reduces triglyceride content in mice fed a low but not high-fat diet. *Biochim. Biophys. Acta* **1851**, 210–219 (2015).
39. Brandon, A. E. et al. Protein kinase C epsilon deletion in adipose tissue, but not in liver, improves glucose tolerance. *Cell Metab.* **29**, 183–191.e7 (2019).
40. Hansotia, T. et al. Double incretin receptor knockout (DIRKO) mice reveal an essential role for the enteroinsular axis in transducing the glucoregulatory actions of DPP-IV inhibitors. *Diabetes* **53**, 1326–1335 (2004).
41. Pal, M. et al. Alteration of JNK-1 signaling in skeletal muscle fails to affect glucose homeostasis and obesity-associated insulin resistance in mice. *PLoS ONE* **8**, e54247 (2013).

Acknowledgements This study was funded, in part, by the National Health & Medical Research Council of Australia (project grant 526606 and APP1156511 to M.A.F. and S.R.-J.; project grant APP1039502 to M.A.F.; development grant APP1039502 to M.A.F., T.E.A. and M.A.C.; principal research fellowship 445302 to M.A.F., senior principal research fellowship (SPRF) APP1021168 to M.A.F. and SPRF APP1116936 to M.A.F. This project was also funded, in part, by a CASS Foundation grant awarded to T.L.A. and M.A.F. and CIHR foundation grant 164321 to D.J.D. The project was also supported in part by the Victorian Government's OIS Program. We thank F. T. Wunderlich and C. M. Wunderlich for providing reagents to generate the ROSA26-IC7Fc mouse, as well as A. Nenci and J. Gonzales from the Monash Gene Targeting Facility. M.P. was supported by a research fellowship (DFG, PA-2459/1-1). We thank J. Scoble and L. Sparrow for their help in preparing PEGylated forms of IC7, J. Bentley for help with europium assays, X. Xiao and G. Lovrecz for mammalian cell line development and scale-up, L. Pontes-Braz for protein purification and the Burnet ImmunoMonitoring Facility for conducting the human PBMC experiments. The work of S.R.-J. was funded by the Deutsche Forschungsgemeinschaft (DFG), Bonn (grant no.: SFB841, project C1; grant no.: SFB877, project A1), and by the Cluster of Excellence 'Inflammation at Interfaces'.

Author contributions M.F. and T.L.A. conducted experiments and performed analyses described in all figures. P.G. and K.I.W. performed YAP1 experiments in Fig. 1. D.C.H., H.K., E.E., C.Y., C.E., S.R., R.S.L., M.J.K., N.A.M., L.M.T., J.S. and E.T.K. conducted experiments and performed analyses for GLP-1RA plus IC7Fc experiments. T.E.A. supplied IC7A, IC7B and IC7Fc and provided the europium binding methodology. L.C. performed western blot analyses. A.E.B. and G.J.C. conducted euglycaemic clamp experiments. G.M.K. and C.R.B. conducted tracer determined OGTT experiments. L.O. and T.J.B. conducted GSIS experiments. E.S., D.J.K. and R.L.Y. performed surgeries, experiments and analyses in GLP-1 secretion from human patient samples. L.L.B. and D.J.D. conducted experiments and performed analyses in GLP-1R knockout mice. M.A.C. co-ordinated non-human primate studies. M.P. generated the ROSA26-IC7Fc mouse. P.J.M. co-ordinated lipidomic experiments. P.A.B. conducted bone density experiments in IC7Fc^{Alb-cre} mice. J.G., C.G. and S.R.-J. made native IC7. G.K., T.E.A., T.L.A. and M.A.F. conceived and synthesized mIC7A, mIC7B and IC7Fc. M.A.F. and S.R.-J. conceived the project. M.A.F., T.L.A. and M.F. wrote the manuscript. M.A.F. co-ordinated all aspects of this work.

Competing interests M.A.F. and S.R.-J. are the inventors of IC7Fc and hold patents for this molecule (US 60/920,822; WO/2008/119110 A1). M.A.F. is the founder and CSO of Kinomedica Pty Ltd. G.K., T.L.A. and S.R.-J. have financial interests in Kinomedica Pty Ltd.

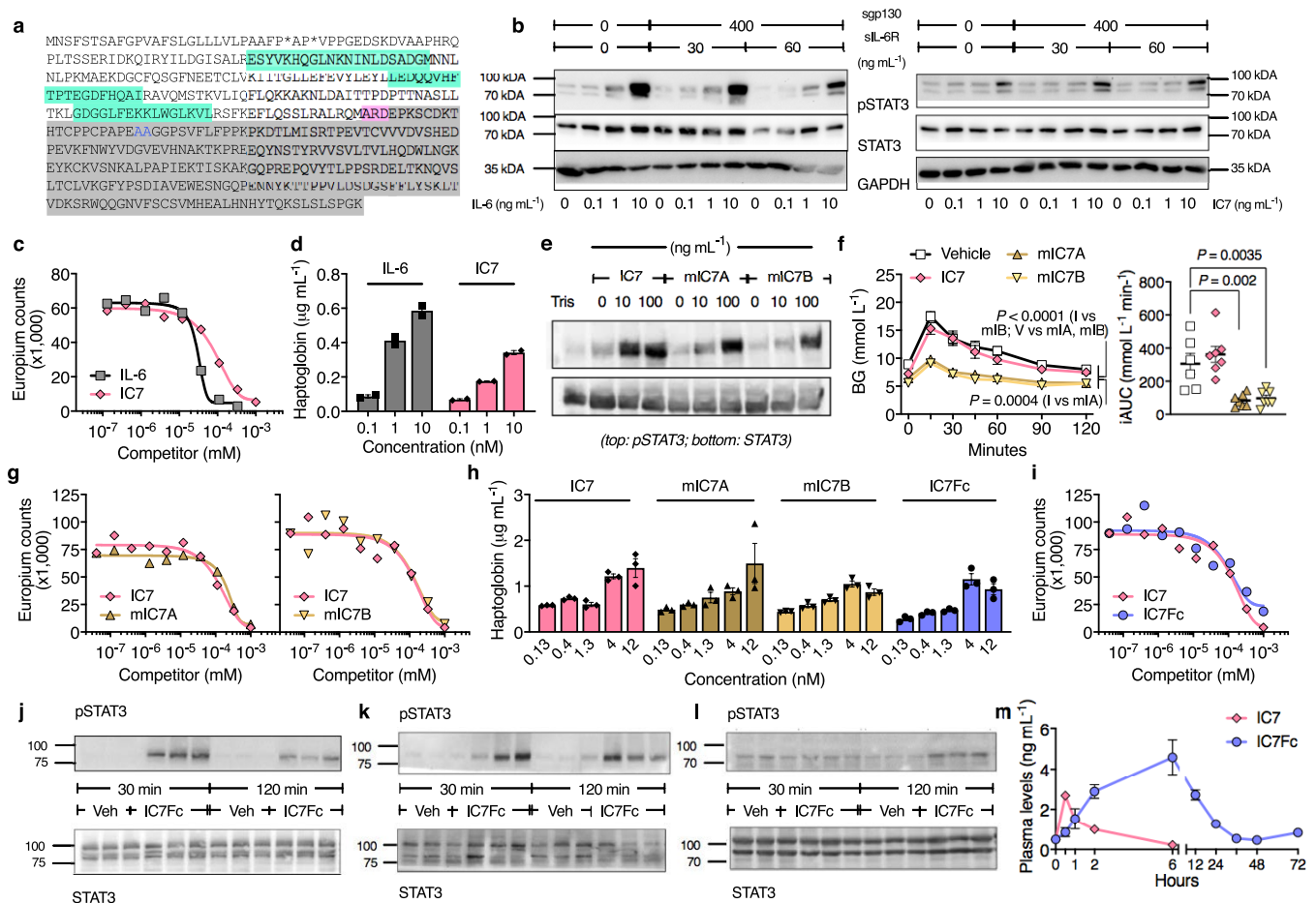
Additional information

Supplementary information is available for this paper at <https://doi.org/10.1038/s41586-019-1601-9>.

Correspondence and requests for materials should be addressed to M.A.F.

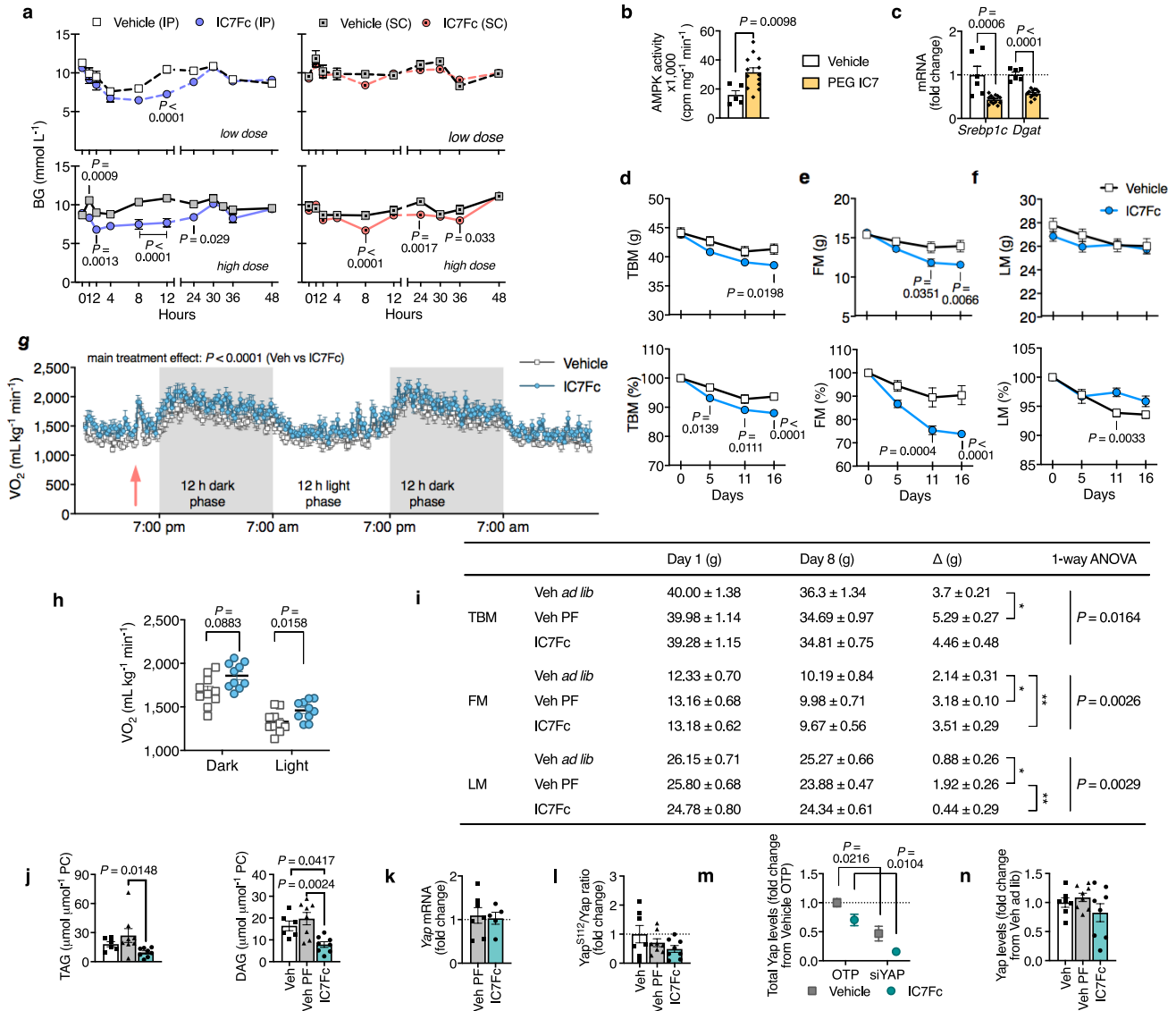
Peer review information *Nature* thanks Marc Donath, Kun-Liang Guan, Barbara Hansen and the other, anonymous, reviewer(s) for their contribution to the peer review of this work.

Reprints and permissions information is available at <http://www.nature.com/reprints>.



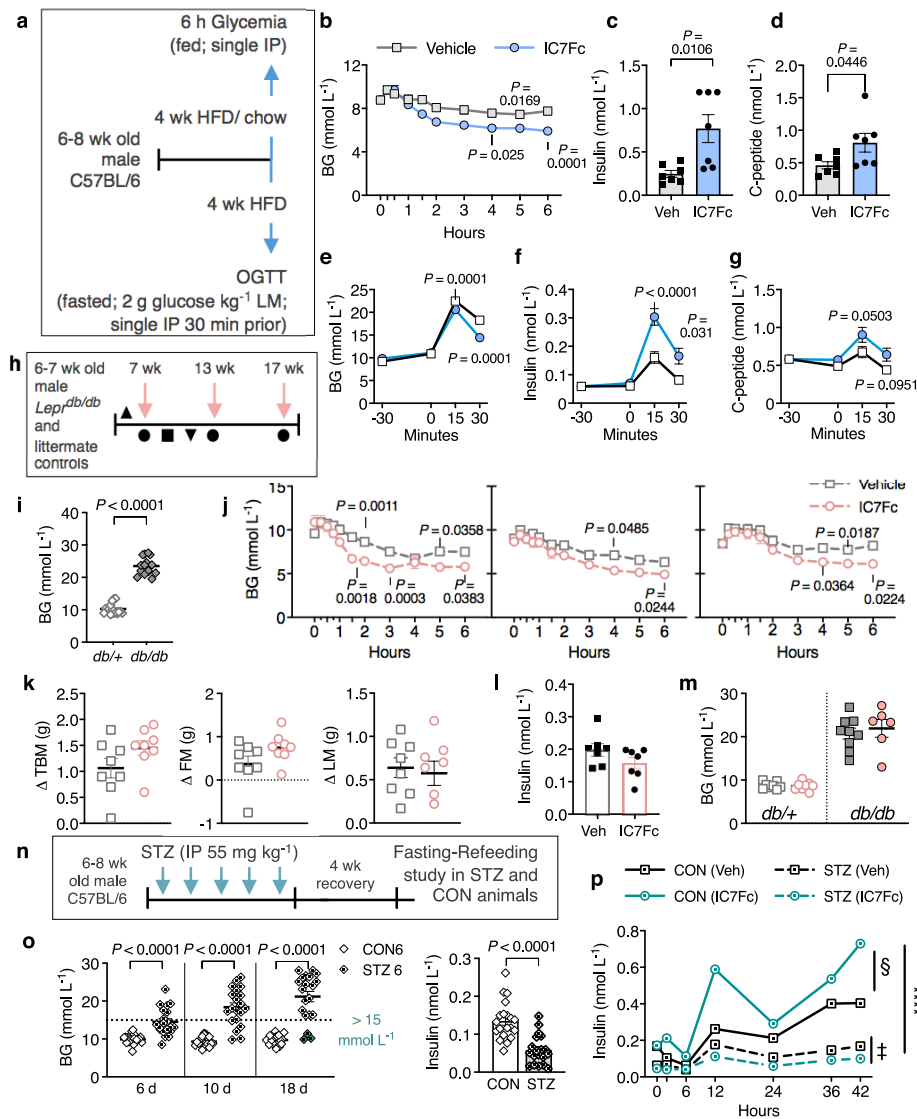
Extended Data Fig. 1 | IC7 can bind and signal in vitro. **a**, Sequence of IC7Fc. Blue shading denote IC7 site 3 loop sequence; magenta shading denote a spacer sequence from the BssHIII restriction site; grey shading denote the Fc fragment sequence; blue residues denote mutated amino acids in the Fc fragment. **b**, HepG2 cells were stimulated with IL-6 (left) or IC7 (right) in the absence or presence of soluble gp130 (sgp130) and low or high doses of soluble IL-6R (sIL-6R). **c**, Ability of IC7 to compete with europium-labelled IL-6 to bind to sgp130 and sIL-6R. **d**, Ability of IC7 to activate gp130 signalling and induce haptoglobin secretion. $n = 3$ technical replicates per condition in **c** and **d**. **e**, pSTAT3 treated with IC7 (lanes 2–4) and PEGylated mIC7A (30 kDa; lanes 5–7) and mIC7B (40 kDa; lanes 8–10). **f**, Mice were fed a HFD for 8 weeks and treated daily with IC7, mIC7A, mIC7B (1 mg kg⁻¹) or vehicle over 8 days. The effects on glucose tolerance in an intraperitoneal glucose tolerance test on day 5 of

the intervention are shown ($n = 7$ for all groups, except $n = 6$ for vehicle). Left, change in blood glucose. Right, incremental area under the curve (iAUC). P value determined by one-way ANOVA with Dunnett's multiple comparison test. **g–i**, Modified and unmodified IC7 were assessed for their ability to compete with europium-labelled IL-6 to bind to the sIL-6R and sgp130 (**g**, **i**) and to induce haptoglobin secretion in HepG2 cells (**h**). **j–l**, C57BL/6 mice were fed a HFD for 4 weeks and injected intraperitoneally with a single dose of vehicle or IC7Fc in the fed state (mice were killed 30 and 120 min after injection), and STAT3 phosphorylation was analysed in liver (**j**), epididymal fat (**k**) and quadriceps muscles (**l**). Blots represent $n = 6$ mice per group. **m**, Pharmacokinetic profile over 72 h in plasma of mice after a single intraperitoneal dose (1 mg kg⁻¹) of IC7 or IC7Fc. Mice were killed after 2, 6, 24, 48 or 72 h ($n = 10$ for IC7 and $n = 25$ for IC7Fc). Data are mean \pm s.e.m. (except in **d**, data are mean \pm s.d.).



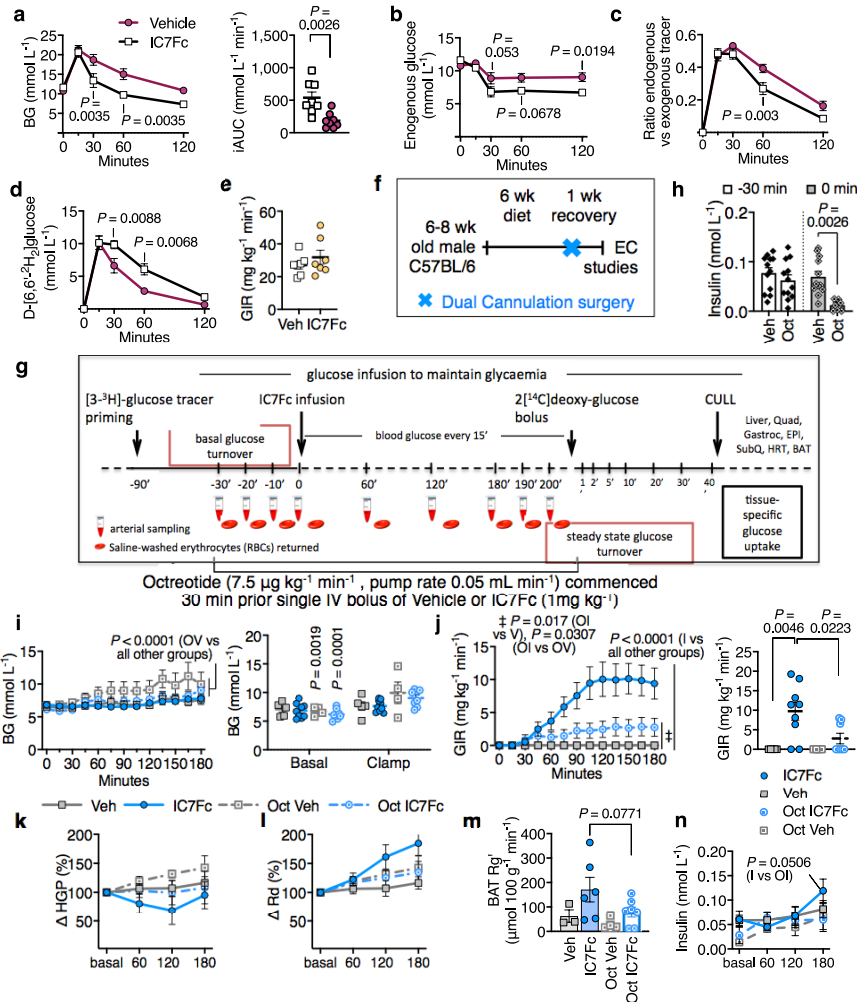
Extended Data Fig. 2 | Effect of IC7Fc on DIO in mice. **a**, Mice received a single escalating dose of IC7Fc (low: 0.1 mg kg⁻¹; high: 1 mg kg⁻¹; $n = 5-25$) or an equal volume of vehicle ($n = 5$), administered either intraperitoneally (IP) or subcutaneously (SC). **b, c**, Liver AMPK activity (b) and mRNA expression of *SREBP1c* and *Dgat1* (c) in DIO mice injected daily for 7 days with vehicle ($n = 6$) or PEGylated (PEG) IC7 (1 mg kg⁻¹, $n = 13$). **d-f**, Sixteen-day intervention study in DIO mice fed a HFD for 8 weeks and injected every other day with vehicle ($n = 7$) or IC7Fc (1 mg kg⁻¹, $n = 8$) for 16 days. Body composition was analysed as follows: change in total mass (top) and as percentage of starting weight (bottom) of total body mass (d), fat mass (e), and lean mass (f) during intervention. **g, h**, Chronically treated mice ($n = 10$ per treatment) were monitored in metabolic cages at 30 °C for 48 h. Oxygen consumption

(VO₂) recorded over 48 h during 13 days and 15 days of intervention (g) and average VO₂ (h) were determined. **i-l**, Raw data of absolute weight changes (i), liver triacylglycerol (TAG; left) diacylglycerol (DAG; right) (j), gastrocnemius *Yap1* mRNA (k) and the ratio of YAP1(Ser112) to YAP1 protein (l) during the paired-feeding study (related to Fig. 1j-l). **m**, Quantification of total YAP1 levels in C2C12 myotubes treated with vehicle or IC7Fc (1 ng ml⁻¹) for 24 h after knockdown of YAP1 (siYAP) or siRNA control (ON-TARGETplus, OTP); $n = 3$. **n**, Quantification of YAP1 protein levels in liver tissue of chronically treated mice. $n = 7$ (Veh), $n = 8$ (Veh PF, IC7Fc) in j-l, n. Data are mean ± s.e.m. *P* values determined by: two-way ANOVA with Sidak's multiple comparison test (a, d-f), multiple *t*-test using the Holm-Sidak method (b, c, h, k, m), or ordinary one-way ANOVA with Tukey's multiple comparison test (g, j, l).



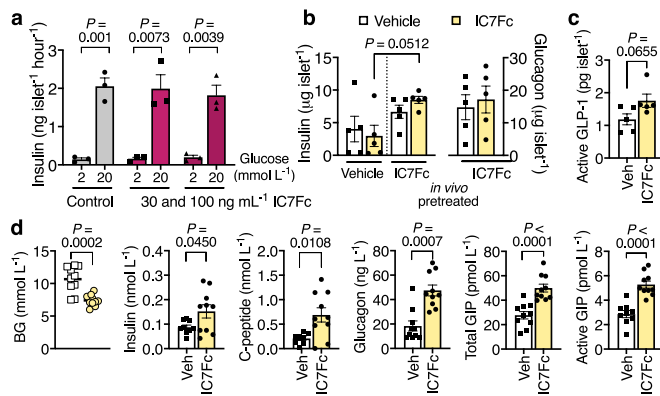
Extended Data Fig. 3 | IC7Fc lowers glucose via increased insulin secretion. **a–g**, Acute metabolic studies in 10–11-week-old C57BL/6 mice. **a**, Study design. **b–d**, Chow-fed mice received a single intraperitoneal dose of vehicle ($n = 13$) or IC7Fc ($n = 14$) in the fed state and blood glucose was monitored over 6 h (**b**). Change in plasma insulin (**c**) and C-peptide (**d**) 2 h after injection ($n = 7$ per treatment). **e–g**, DIO mice were fasted for 6 h and injected intraperitoneally with vehicle or IC7Fc 30 min before an OGTT. Mice were killed at -30, 0, 15 and 30 min, respectively. Changes in plasma blood glucose (**e**), insulin (**f**) and C-peptide (**g**) were determined. $n = 16–25$ (**e**), $n = 15–22$ (**f**), $n = 15–23$ mice (**g**); for details, see Source Data. **h–m**, Acute metabolic studies in the genetically obese leptin receptor-deficient (*Lep^{db/db}*) mouse model. **h**, Study design. **i**, Blood glucose levels in fed 7-week-old mice; $n = 16$ (*db/+*), $n = 15$ (*db/db*). **j**, Blood glucose levels after a single intraperitoneal dose of vehicle or IC7Fc (1 mg kg⁻¹) in control mice (*db/+*) at the age of 7 weeks (left), 13 weeks (middle) and 17 weeks (right); $n = 8$ (per treatment). **k**, Body composition analysed as weight changes in total body mass (left), fat mass (middle) and lean mass (right) 10 days after a single injection in *db/+* mice ($n = 8$). **l**, Change in fasting plasma insulin in *db/+* mice 17 days after treatment ($n = 7$ per group). **m**, Change in fasting blood glucose in *db/db*

($n = 8$ each treatment) and *db/+* mice with treated with vehicle ($n = 9$) or IC7Fc ($n = 6$), 17 days after injection. **n–p**, Acute studies in chemically induced model of diabetes. Six-to-seven-week-old male mice were injected intraperitoneally with either placebo (CON) or STZ (55 mg kg⁻¹) over five consecutive days to induce diabetes ($n = 20$ per group). **n**, Study design. **o**, Fasting blood glucose and insulin levels in control and STZ mice 6, 10 and 18 days after induction. Left, STZ mice with fasting blood glucose below 15 mM (highlighted in blue) were excluded from the study. Right, corresponding fasting insulin in control and STZ mice ($n = 17$) 10 days after induction. **p**, Change in plasma insulin over 42 h; $n = 10$ CON (all groups), $n = 9$ STZ (Veh) and 8 STZ (IC7Fc). Data are mean \pm s.e.m. P values were determined by: two-way ANOVA with Sidak's multiple comparison test (**b**, **e–g**, **j**; IC7Fc versus Veh at indicated time points); two-tailed unpaired Mann–Whitney *U*-test (**c**), Student's two-tailed unpaired *t*-test (**d**, **i**, **k–m**, **o**); ordinary two-way ANOVA with Tukey's multiple comparison test for main treatment effect (**p**). **** $P < 0.0001$ for STZ (Veh) versus CON (Veh), STZ (Veh) versus CON (IC7Fc), STZ (IC7Fc) versus CON (Veh), STZ (IC7Fc) versus CON (IC7Fc); § $P = 0.0062$ for STZ (Veh) versus STZ (IC7Fc); ‡ $P = 0.0104$ for CON (Veh) versus CON (IC7Fc).

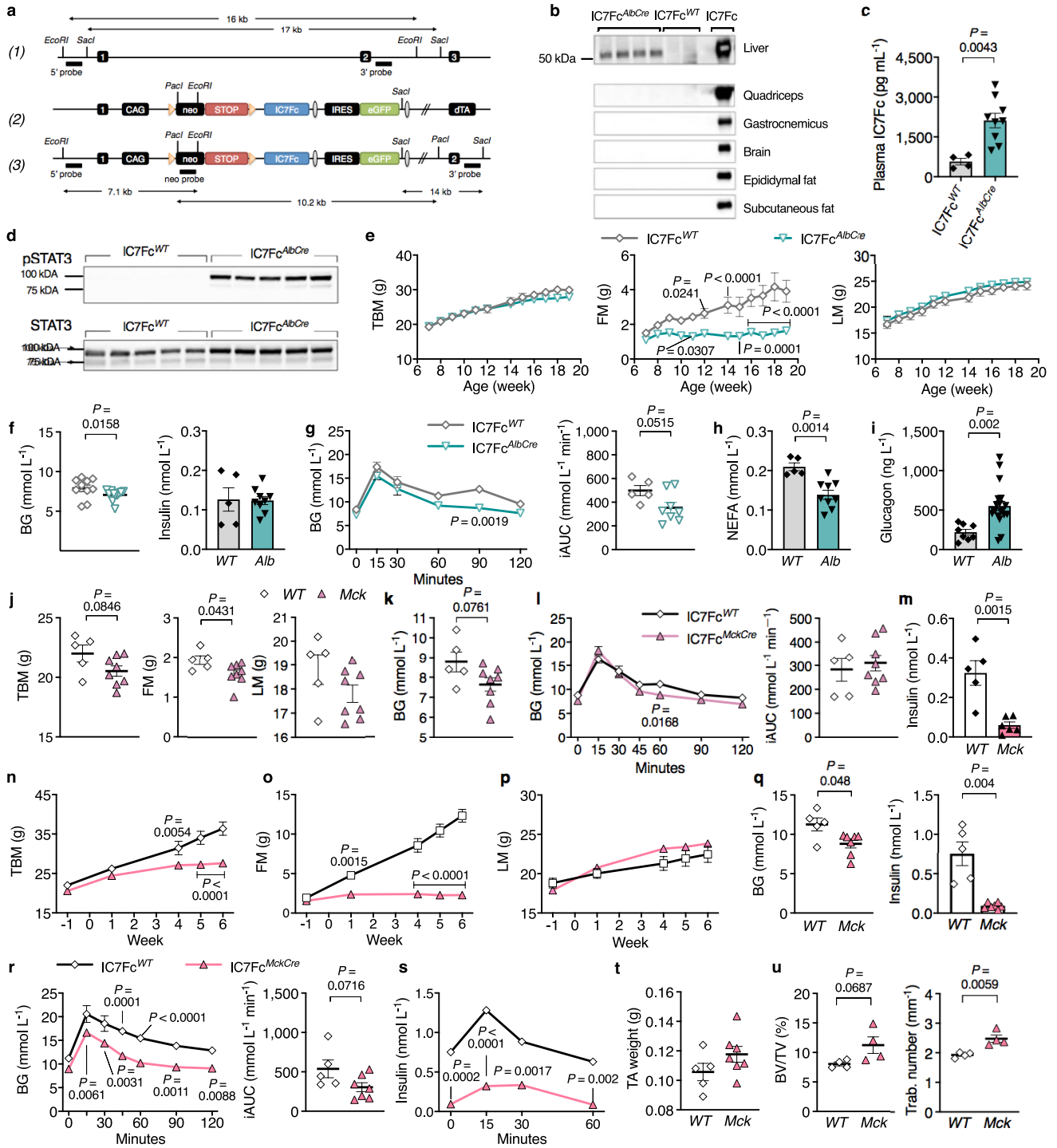


Extended Data Fig. 4 | IC7Fc suppresses glucose production and increases glucose disposal. **a–d**, Stable isotope tracer studies in DIO mice treated with vehicle or IC7Fc (1 mg kg⁻¹) 30 min before an OGTT using D-[6,6'-²H₂]glucose (*n* = 8 per group). Blood glucose (**a**, left) and iAUC (**a**, right), proportion of blood glucose from hepatic glucose production (**b**), the ratio of exogenous (tracer) and endogenous (hepatic) glucose (that is, tracer enrichment) (**c**), and D-[6,6'-²H₂]glucose (**d**) during the OGTT. **e**, GIR during an euglycaemic–hyperinsulinaemic clamp in vehicle- or IC7Fc-injected mice (*n* = 7 each group). **f–n**, Euglycaemic clamp (EC) studies in DIO and chow-fed mice with intravenous bolus injections of vehicle or IC7Fc in the presence and absence of constant octreotide infusion (7.5 μg kg⁻¹ min⁻¹). **f**, Study design. **g**, Experimental protocol. **h**, Insulin levels in the basal period of the clamp before and after octreotide or vehicle infusion (*n* = 12). **i–n**, Euglycaemic clamp experiments in 14–16-week-old chow-fed mice; *n* = 5 (Veh), *n* = 9 (IC7Fc), *n* = 4 (Oct

Veh), *n* = 8 (Oct IC7Fc). **i**, **j**, Blood glucose levels (**i**) and GIR (**j**) over time (left) and before and after clamp (right). **k**, **l**, Change in HGP (**k**) and glucose turnover (Rd; **l**) during the euglycaemic clamp. Data are normalized and expressed as percentage of basal levels. **m**, Glucose uptake (Rg') in BAT; *n* = 3 (Veh), *n* = 6 (IC7Fc), *n* = 4 (Oct Veh), *n* = 7 (Oct IC7Fc). **n**, Insulin levels throughout the clamps. Data are mean ± s.e.m. *P* values were determined by: two-way ANOVA with Sidak's multiple comparison test (**a–d**, **g**, **i** (right); between basal and clamp); **k**, **l**, **n** (between groups at time points)); multiple comparison test using the Holm–Sidak method (Veh versus Oct –30 and 0 min in **h**); two-way ANOVA with Tukey's multiple comparison test (main treatment effect in **i** (left) and **j** (left)); ordinary one-way ANOVA with Tukey's multiple comparisons test (**i** (right); between groups)); nonparametric Kruskal–Wallis test and Dunn's multiple comparison test (**m**).



Extended Data Fig. 5 | Effect of IC7Fc on insulin secretion and hormonal milieu. **a**, GSIS in pancreatic islets isolated from 10-week-old normal chow-fed mice. Stimulation with saline (control) or IC7Fc (30 or 100 ng mL⁻¹), in the presence of 2 or 20 mM glucose. $n = 3$ replicates in three independent experiments. **b–d**, DIO mice intraperitoneally injected daily with vehicle or IC7Fc (1 mg kg⁻¹) over 8 days in week 8 during high-fat feeding ($n = 10$ mice per group). Mice were killed in the fed state 2 h after the last intraperitoneal injection. **b**, **c**, Pancreatic islets were isolated from DIO mice that had been injected daily. Insulin and glucagon content (**b**) and active GLP-1 (**c**) were determined in isolated islets from five mice per group; **b**, left, three to four technical replicates; right, two independent experiments; **c**, two technical replicates except one Veh mouse. **d**, Blood glucose, insulin, C-peptide, glucagon, total and active GIP (1–42); $n = 10$ (Veh), $n = 10$ (IC7Fc), except $n = 9$ (Veh) for insulin and active GIP, $n = 8$ (Veh) for C-peptide. P values determined by: multiple two-tailed t -test (**a**); ordinary one-way ANOVA followed by Sidak's multiple comparisons test (**b** (left)); Student's two-tailed unpaired t -test (**b** (right), **c** and **d**); or two-tailed unpaired Mann–Whitney U -test (**d**, glucagon).

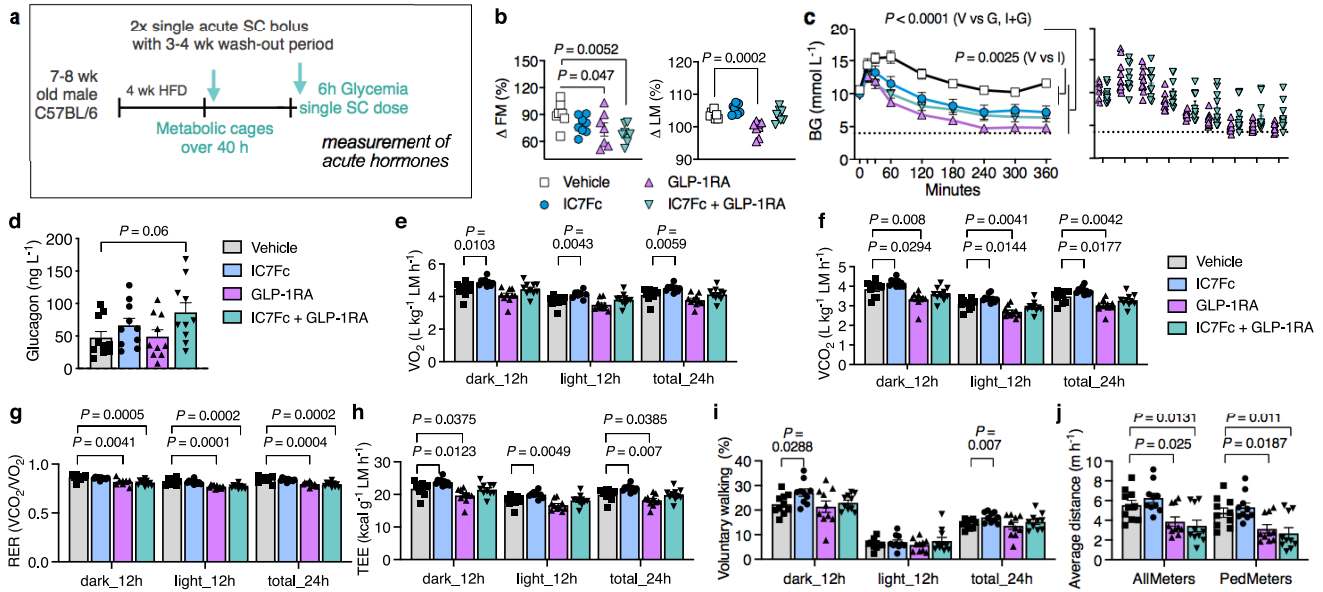


Extended Data Fig. 6 | See next page for caption.

Extended Data Fig. 6 | Generation and phenotype of mice

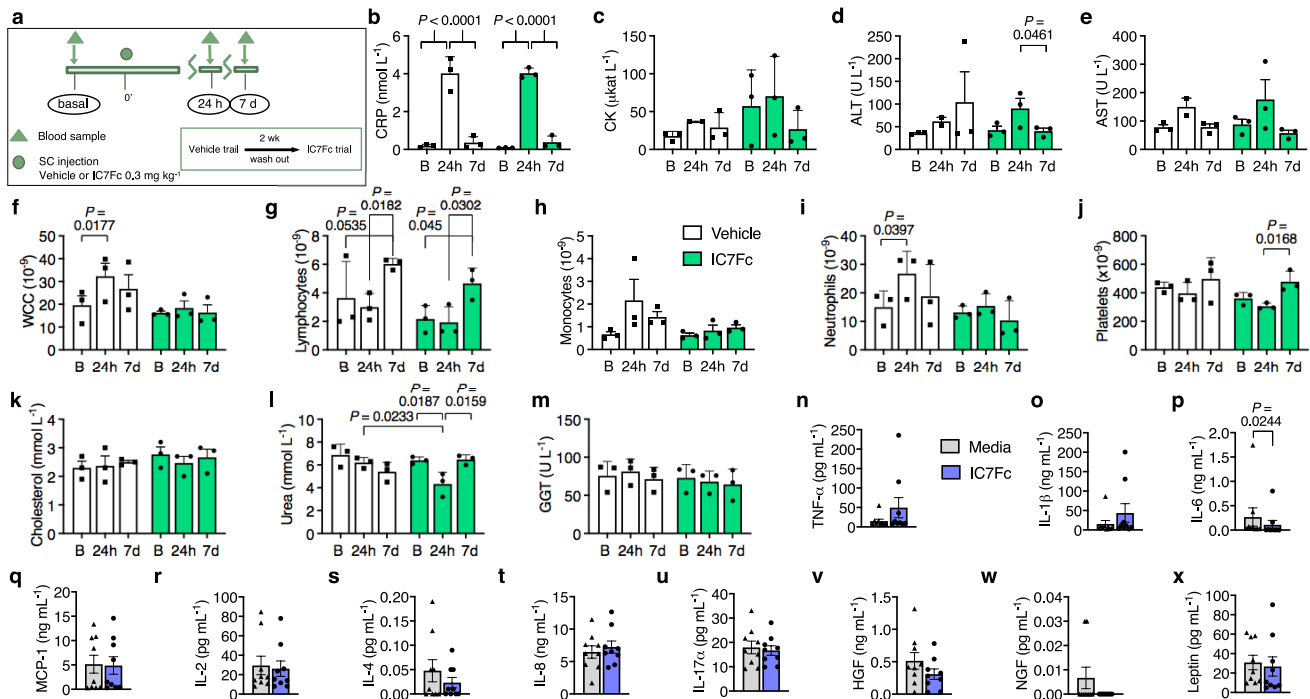
overexpressing IC7Fc. **a**, Schematic describing the generation of ROSA26-IC7Fc mice. The panel shows (1) ROSA26 wild-type locus; (2) ROSA26-IC7Fc targeting vector; and (3) ROSA26 locus after homologous recombination. **b–d**, Eight-week-old male mice that overexpress liver-specific IC7Fc (IC7Fc^{Alb-cre}) and littermate controls (IC7Fc^{WT}) were killed in the fed state. IC7Fc expression was determined by western blots in different tissues (**b**) and circulating IC7Fc levels in plasma were detected by ELISA (**c**); $n = 4$ (WT), $n = 9$ (*Alb*). **d**, STAT3 phosphorylation in liver tissues from IC7Fc^{Alb-cre} mice. **e–i**, Eight-week-old IC7Fc^{Alb-cre} and control (IC7Fc^{WT}) mice fed a chow diet until 19 weeks of age. **e**, Growth curve as change in total body mass (left), fat mass (middle) and lean mass (right) of chow-fed IC7Fc^{Alb-cre} mice ($n = 9$) and littermate controls ($n = 5$). **f**, Fasting blood glucose (left) and insulin levels (right) in 8-week-old mice; left, $n = 10$ and 12, and right, $n = 5$ and 9 for WT and *Alb* mice, respectively. **g**, Glucose levels during an OGTT shown as time course (left) and expressed as iAUC (right) in fasted mice; $n = 5$ (WT), $n = 8$ (*Alb*). **h, i**, Plasma levels of NEFA and glucagon in 19-week-old transgenic mice; $n = 5$ and 9 (**h**) and $n = 8$ and 19 (**i**) for WT and *Alb* mice, respectively. **j–t**, Differences between 7-week-old male IC7Fc^{MCK-cre} mice (MCK,

$n = 8$)—which predominantly overexpress muscle-specific IC7Fc (mice were kept at 30 °C holding temperature)—and littermate control mice (WT, $n = 5$), before the start of diet intervention. **j**, Total body mass, fat mass and lean mass. **k**, Fasting blood glucose. **l**, Glucose levels during an OGTT shown as time course (left) and expressed as iAUC (right). **m**, Fasting insulin levels after a 4-week HFD in IC7Fc^{MCK-cre} mice ($n = 6$) and littermate controls ($n = 5$). **n–t**, Eight-week-old IC7Fc^{MCK-cre} mice ($n = 5$) and littermate controls ($n = 7$) fed a HFD for 6 weeks. Total body mass (**n**), fat mass (**o**) and lean mass (**p**). Fasting blood glucose levels (**q**, left), insulin levels (**q**, right), glucose during an OGTT (**r**) and plasma insulin (**s**) after a HFD. **t**, Difference in weight of tibialis anterior (TA) of mice at cull at 14 weeks of age. **u**, Normal chow-fed 26-week-old male IC7Fc^{MCK-cre} and littermate mice were kept at 22 °C holding temperature ($n = 4$ per genotype) and femurs were analysed as follows: Percentage of BV/TV (left) and quantification of trabecular number (right). Data are mean \pm s.e.m. *P* values determined by: Student's two-tailed unpaired *t*-test (**c, f** (right), **g–m, q** (right), **r, t, u**); two-tailed unpaired Mann–Whitney *U*-test (**f** (left) and **q** (left)); two-way ANOVA with Sidak's multiple comparisons test (**e, g, l, n–p, r, s**).



Extended Data Fig. 7 | IC7Fc reverses some of the unwanted side effects of GLP-1RA treatment. Effects of a single injection of vehicle, IC7Fc (1 mg kg^{-1}), dulaglutide (GLP-1RA; 0.5 mg kg^{-1}) or a combination of the latter (IC7Fc + GLP-1RA) on body mass, energy homeostasis and metabolism in DIO mice; $n = 10$ mice per treatment unless specified otherwise. **a**, Study design. **b**, Percentage change in fat mass (left) and lean mass (right) 5–7 days after injection ($n = 8$ per group, except $n = 7$ for GLP-1RA). **c**, Glycaemia in fed mice shown as mean blood glucose (left) and as stratified data points (right) in mice after acute injection over time. **d**, Circulating plasma glucagon at cull 6 h after injection. **e–h**, Oxygen

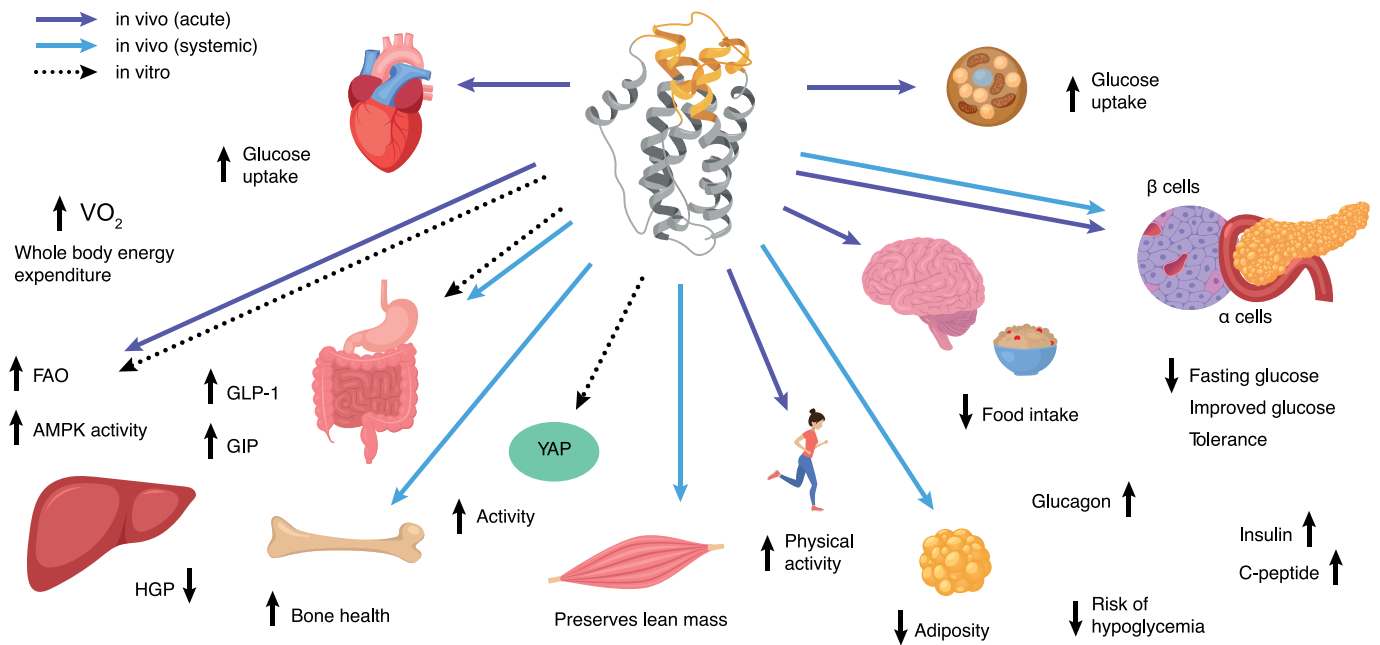
consumption (VO_2 , **e**) carbon dioxide production (VCO_2 , **f**), respiratory exchange ratio (RER, **g**) and total energy expenditure (TEE, **h**). **i**, Physical activity of mice analysed as percentage of time spent voluntary walking and presented as average of a 12-h dark or light phase and 24-h recording period. **j**, Physical activity as average value of measurements made within the 8 h of the first dark phase flanking 07:00. Data are mean \pm s.e.m. P values determined by ordinary one-way ANOVA with Dunnett's multiple comparisons test (**b**, **d**); two-way ANOVA with Dunnett's multiple comparison test (**c**); or multiple two-tailed t -tests (**e–j**).



Extended Data Fig. 8 | Safety profile of IC7Fc. **a–g**, Acute study in non-human primates (cynomolgus macaques); $n = 3$ unless specified otherwise. **a**, Study design. **b–m**, Markers of inflammation in blood samples 24 h and 7 days after treatment were analysed as follows: changes in C-reactive protein (CRP, **b**), creatine kinase (CK, **c**, $n = 2$ for 24 h Veh), in alanine aminotransferase (ALT, **d**, $n = 2$ for 24 h Veh), aspartate aminotransferase (AST, **e**, $n = 2$ for 24 h Veh), white blood cell count (WCC, **f**), lymphocytes (**g**), monocytes (**h**), neutrophils (**i**), platelets (**j**), cholesterol (**k**), urea (**l**) and gamma-glutamyltransferase (GGT, **m**). **o–x**, Human PBMCs were cultured for 48 h with medium, IC7Fc

($3 \mu\text{g ml}^{-1}$) or PHA ($5 \mu\text{g ml}^{-1}$); $n = 9$. Supernatant was analysed as follows: TNF (**n**), IL-1 β (**o**), IL-6 (**p**), MCP-1, **q**), IL-2 (**r**), IL-4 (**s**), IL-8 (**t**), IL-17 α (**u**), hepatocyte growth factor (HGF, **v**), nerve growth factor (NGF, **w**) and leptin (**x**). P values were determined by: two-way ANOVA (**b**, **f–m**) or mixed effects model (**c–e**), with Sidak's multiple comparison test for differences between treatment at time points, and Tukey's multiple comparison test to detect differences in-between time points for one condition; Student's two-tailed unpaired t -test (**q**, **s–x**); or non-parametric two-tailed unpaired Mann–Whitney U -test (all other panels) comparing IC7Fc and medium only. See Source Data for PHA.

Summary of the metabolic actions of IC7Fc



Extended Data Fig. 9 | Graphical summary of the metabolic actions of IC7Fc. IC7Fc has several beneficial actions on metabolic processes.

Extended Data Table 1 | Raw data for euglycaemic clamp experiments

		HFD				Chow			
		Vehicle		IC7Fc		Vehicle		IC7Fc	
		- Oct	- Oct	+ Oct	+ Oct	- Oct	- Oct	+ Oct	+ Oct
HGO (mg min ⁻¹ kg ⁻¹)	basal	14.64 ± 1.9	14.04 ± 1.67	10.28 ± 0.88	10.65 ± 1.14	10.23 ± 1.37	10.52 ± 1.16	11.3 ± 1.57	11.36 ± 1.28
	60 min	14.5 ± 1.75	10.62 ± 2.15	13.09 ± 0.82	12.4 ± 0.96	10.47 ± 0.84	8.34 ± 1.45	13.17 ± 1.09	11.29 ± 1.6
	120 min	14.78 ± 1.15	9.96 ± 1.6	12.49 ± 0.99	12.14 ± 0.78	10.44 ± 1.04	5.42 ± 1.95	14.62 ± 1.32	10.86 ± 2.12
	180 min	14.4 ± 1.21	12.86 ± 1.72	13.85 ± 0.47	13.14 ± 0.82	11.67 ± 1.35	8.4 ± 1.81	15.35 ± 1.17	11.37 ± 2.75
Rd (mg min ⁻¹ kg ⁻¹)	basal	14.64 ± 1.9	14.04 ± 1.67	10.28 ± 0.88	10.65 ± 1.14	10.23 ± 1.37	10.52 ± 1.16	11.3 ± 1.57	11.36 ± 1.28
	60 min	14.5 ± 1.75	16.27 ± 2.19	13.09 ± 0.82	12.4 ± 0.96	10.47 ± 0.84	12.02 ± 0.77	13.17 ± 1.09	12.45 ± 1.06
	120 min	14.78 ± 1.15	19.51 ± 1.86	12.49 ± 0.99	12.14 ± 0.78	10.44 ± 1.04	15.48 ± 1.29	14.62 ± 1.32	13.3 ± 1.08
	180 min	14.4 ± 1.21	21.01 ± 2.21	13.85 ± 0.47	13.14 ± 0.82	11.67 ± 1.35	17.89 ± 1.24	15.35 ± 1.17	14.12 ± 1.54
Rg' (μmol 100g ⁻¹ min ⁻¹)	Skeletal muscles	21.64 ± 3.71	25.81 ± 4.24	22.82 ± 4.28	17.92 ± 2.7	10.96 ± 2.2	26.17 ± 2.74	21.36 ± 3.05	30.6 ± 5.39
	White adipose tissue	1.04 ± 0.12	0.91 ± 0.16	0.67 ± 0.13	0.79 ± 0.09	2.33 ± 0.75	2.56 ± 0.57	2.07 ± 0.6	2.37 ± 0.36
	Brain	19.77 ± 3.67	17.27 ± 1.5	17.22 ± 1.57	21.59 ± 1.48	15.97 ± 1.76	17.66 ± 1.27	14.86 ± 1.94	18.52 ± 0.75
	Heart	N/A	47.0 ± 20.27 *	10.43 ± 2.73	12.34 ± 2.61	15.97 ± 1.76	15.9 ± 6.07	11.26 ± 3.24	13.63 ± 4.84

Mice fed a standard chow diet or HFD for 6 weeks were treated with vehicle or IC7Fc (1 mg kg⁻¹), in the presence (+Oct) and absence (-Oct) of octreotide (7.5 μg kg⁻¹ min⁻¹) in mice. All data are mean ± s.e.m. **P* = 0.08 for IC7Fc versus octreotide IC7Fc (glucose uptake into heart within HFD group), Kruskal-Wallis test with Dunn's multiple comparison test. N/A, not available.

Reporting Summary

Nature Research wishes to improve the reproducibility of the work that we publish. This form provides structure for consistency and transparency in reporting. For further information on Nature Research policies, see [Authors & Referees](#) and the [Editorial Policy Checklist](#).

Statistical parameters

When statistical analyses are reported, confirm that the following items are present in the relevant location (e.g. figure legend, table legend, main text, or Methods section).

n/a Confirmed

- The exact sample size (n) for each experimental group/condition, given as a discrete number and unit of measurement
- An indication of whether measurements were taken from distinct samples or whether the same sample was measured repeatedly
- The statistical test(s) used AND whether they are one- or two-sided
Only common tests should be described solely by name; describe more complex techniques in the Methods section.
- A description of all covariates tested
- A description of any assumptions or corrections, such as tests of normality and adjustment for multiple comparisons
- A full description of the statistics including central tendency (e.g. means) or other basic estimates (e.g. regression coefficient) AND variation (e.g. standard deviation) or associated estimates of uncertainty (e.g. confidence intervals)
- For null hypothesis testing, the test statistic (e.g. F , t , r) with confidence intervals, effect sizes, degrees of freedom and P value noted
Give P values as exact values whenever suitable.
- For Bayesian analysis, information on the choice of priors and Markov chain Monte Carlo settings
- For hierarchical and complex designs, identification of the appropriate level for tests and full reporting of outcomes
- Estimates of effect sizes (e.g. Cohen's d , Pearson's r), indicating how they were calculated
- Clearly defined error bars
State explicitly what error bars represent (e.g. SD, SE, CI)

Our web collection on [statistics for biologists](#) may be useful.

Software and code

Policy information about [availability of computer code](#)

Data collection	Comprehensive Laboratory Animal Monitoring System (CLAMS/Oxymax, Columbus Instruments, Version 4.85).
Data analysis	Statistical analyses - GraphPad Prism (version 7.0d and 8 for Mac OS X, GraphPad Software, La Jolla California USA). Human PBMC multiplex analysis -Bio-Plex Manager 5.0 and Excel (version 15). Densitometry - ImageJ (Version 1.52f with Java 1.8.0_172 (64bit) (NIH) software (http://rsb.info.nih.gov/ij/index.html) or Bio-Rad Quantity One 1-D (Version 4.5.2). Lipidomics - Multiquant v1.2. MicroCT-images - NRecon (software version 1.6.10.5 (Bruker, Belgium), CTAnalyser software (software version 1.16.1.0, Bruker, Belgium).

For manuscripts utilizing custom algorithms or software that are central to the research but not yet described in published literature, software must be made available to editors/reviewers upon request. We strongly encourage code deposition in a community repository (e.g. GitHub). See the Nature Research [guidelines for submitting code & software](#) for further information.

Data

Policy information about [availability of data](#)

All manuscripts must include a [data availability statement](#). This statement should provide the following information, where applicable:

- Accession codes, unique identifiers, or web links for publicly available datasets
- A list of figures that have associated raw data
- A description of any restrictions on data availability

Data availability

The data supporting the findings of this study are available within the article and its Supplementary Information files, and from the corresponding author upon reasonable request.

Field-specific reporting

Please select the best fit for your research. If you are not sure, read the appropriate sections before making your selection.

Life sciences Behavioural & social sciences Ecological, evolutionary & environmental sciences

For a reference copy of the document with all sections, see [nature.com/authors/policies/ReportingSummary-flat.pdf](https://www.nature.com/authors/policies/ReportingSummary-flat.pdf)

Life sciences study design

All studies must disclose on these points even when the disclosure is negative.

Sample size	In general and based on our experiences using G*POWER 3.1 software (Faul et al. 2009), groups of 8–12 mice are sufficient to detect changes with a power of 80% and statistical significance (alpha level 0.05) for most metabolic parameters (body fat content, circulating glucose and insulin concentrations, food intake, energy expenditure and glucose infusion rate (GIR) during clamp study).
Data exclusions	Pre-specified exclusion criteria were weight loss >10% of initial body weight or signs of illness or injury requiring euthanasia (clamp studies), incorrect gavaging/IP injections during OGTT in animal. Additionally, the exclusion of mathematical proven outliers (formula “average+/- 2x SD”, which allows for exclusion of data greater than 2 standard deviations from mean) was made in the pair feeding study and in the analysis of monkey samples (for AST, ALT, CK). We had to exclude plasma samples if they were hemolyzed and couldn't be analyzed by ELISA. STZ study with stratified BG in order to only include diabetic mice in subsequent studies – criteria: Diabetic OR Significant Postprandial Impairment OR Minor postprandial impairment (all mice included > 15 mmol/L blood glucose). For human GLP-1 secretion experiments only samples that show positive response to at least one positive control (70 mM KCl or 10 μM IBMX/FSK) were included in analysis.
Replication	All experimental findings were reliably reproduced. Non-reproduced studies are: CLAMS, Clamp studies, studies in incretin-receptor deficient mice, db/db mice studies, Chronic and acute side-by-side comparison (Fig 5) For GSIS experiments batches of 5 islets were selected, with at least 6 replicates per group. For in vitro experiments in C2C12 cells: Average myofiber width was determined by measuring fibre width 5-10 times randomly along the length of a myofiber. At least 6 myofibers were measured per field of view in a total of 3-4 independent fields of view per condition.
Randomization	For weight loss experiments in mice were randomly assigned in treatment groups in a manner that resulted in equivalent mean. For chronic studies mice with smaller body weight were assigned to the placebo group, which impacts on body weight the least. remaining mice assigned randomly. Mice were allocated to groups based on their genotype.
Blinding	Investigators were not always able to be blinded due to limitations in available personnel. Investigators administering compounds to animals or cells were not blinded as they were responsible for compound dilutions. Personnel collecting and analyzing data from cells and animals were blinded where possible. Due to the marked effect of the compounds on some metabolic parameters in certain experiments, blinded investigators were able to reasonably predict treatment group assignment as they had prior knowledge of the drug effects.

Reporting for specific materials, systems and methods

Materials & experimental systems

n/a	Involvement	Included
<input type="checkbox"/>	<input checked="" type="checkbox"/>	Unique biological materials
<input type="checkbox"/>	<input checked="" type="checkbox"/>	Antibodies
<input type="checkbox"/>	<input checked="" type="checkbox"/>	Eukaryotic cell lines
<input checked="" type="checkbox"/>	<input type="checkbox"/>	Palaeontology
<input type="checkbox"/>	<input checked="" type="checkbox"/>	Animals and other organisms
<input type="checkbox"/>	<input checked="" type="checkbox"/>	Human research participants

Methods

n/a	Involvement	Included
<input checked="" type="checkbox"/>	<input type="checkbox"/>	ChIP-seq
<input checked="" type="checkbox"/>	<input type="checkbox"/>	Flow cytometry
<input checked="" type="checkbox"/>	<input type="checkbox"/>	MRI-based neuroimaging

Unique biological materials

Policy information about [availability of materials](#)Obtaining unique materials

Antibodies

Antibodies used

Westerns: pStat3 (Tyr705) Ab (# 9131, Cell signaling), lot number 30, 1/1000. pSTAT3 (Y705) (#9145 Cell signaling, Clone D3A7) 1/1000, STAT3 (#9139, Cell Signaling, clone 124H6) 1/1000, GAPDH (#2118, Cell Signaling, clone 14C10) 1/1000. STAT3 (06-596, Upstate, Millipore, Billerica, MA, USA) 1/1000, B actin (cat no), 1/1000, Goat anti Rat IgG-HRP (sc-2065, Santa Cruz)1/2000, Donkey a-goat HRP conjugated (sc-2020, Santa Cruz)1/2000, Anti-rabbit IgG, HRP-linked Antibody (#7074, Cell Signaling), Total YAP (Cell signaling #14074), lot 2, 1/1000. Phosphorylated YAPSer127 (Cell Signaling technologies #4911), lot 5, 1/1000. Goat anti-rabbit (#1706516, Bio-Rad technologies, 1/5000 dilution). IHC: primary antibody against sarcomeric myosin (MF-20; Developmental Studies Hybridoma Bank; 1/50 dilution), secondary antibody (Alexa Fluor 555 conjugated goat anti-mouse IgG2b (A21147; Life Technologies; 1/500 dilution). ELISA - anti-human IL-6 antibody (AB-206-NA, R&D systems, lot no AQ13), 2ug/mL. h-IL-6 Purified Clone MQ2-13A5 (14-7069-85, eBioscience), 0.5ug/mL. Goat anti Rat IgG-HRP (sc-2065, Santa Cruz).

Validation

pSTAT3 - (Tyr705) antibody detects endogenous levels of Stat3 only when phosphorylated at Tyr705. The antibody does not cross-react with other Stat proteins when phosphorylated on the corresponding tyrosine residue. Gels run with canonical activator of STAT3 and blots only contained a single band. Total STAT3 - always run simultaneously with pSTAT3 and blots analysed side by side for band comparison. The Yap blots have positive controls (mouse muscles treated with AAV vectors expressing Yap) loaded on the gels. The antibodies previously used (Watt Kl et al 2015 Nature Comms.) in mouse limb muscles expressing AAV:Yap and Yap shRNA validating their specificity. MF-20 antibody has been used extensively in the field (>15 years). IL6 antibodies were validated on westerns by running recombinant protein on the gel with samples. The ELISA method using IL6 antibodies was optimized prior to sample analysis.

Eukaryotic cell lines

Policy information about [cell lines](#)

Cell line source(s)

C2C12s (CRL-1772, ATCC) HepG2 (HB-8065, ATCC). MIN6 cells were a gift from Eiji Yamato (described in Miyazaki et al, Endocrinology, 1990;127(1):126-32). CHOK1SV (Lonza (RRID:CVCL_DR95) supplied under a research-only licensing agreement).

Authentication

No authentication on cell lines was performed

Mycoplasma contamination

All cell lines listed above were tested and were negative for mycoplasma

Commonly misidentified lines (See [ICLAC](#) register)

Name any commonly misidentified cell lines used in the study and provide a rationale for their use.

Animals and other organisms

Policy information about [studies involving animals](#); [ARRIVE guidelines](#) recommended for reporting animal research

Laboratory animals

C57BL/6 (male, 6-8 weeks), BKS.Cg-Dock7m+/+Leprdb/db & Leprdb(male, 7 weeks), C57BL/6 DIRKO+/+ & DIRKO+/- (male, 6 weeks). C57BL/6-ROSA26-IC7Fc mice, IC7FcAlbCre, IC7FcWT, IC7FcMCKCre (male and female, followed 6-20 weeks) . Non-human primate – Long tail Macaque Cynomolgus Macaque (male, 7-10 years).

Wild animals

Provide details on animals observed in or captured in the field; report species, sex and age where possible. Describe how animals were caught and transported and what happened to captive animals after the study (if killed, explain why and describe method; if released, say where and when) OR state that the study did not involve wild animals.

Field-collected samples

For laboratory work with field-collected samples, describe all relevant parameters such as housing, maintenance, temperature, photoperiod and end-of-experiment protocol OR state that the study did not involve samples collected from the field.

Human research participants

Policy information about [studies involving human research participants](#)

Population characteristics

Participants from which colon mucosae samples were collected were male and female (9/1), aged 52-93 with BMI 22-50. Patients were presenting for bowel resection for cancer. Morphologically normal colonic tissue samples were obtained from sites at least 10 centimetres away from the tumour location of the resected specimen. There are several reports of markedly altered gut hormone secretion in individuals with inflammatory bowel diseases (10.1152/ajpregu.2000.278.4.R1057, 10.1016/j.clnu.2012.08.024, 10.1136/gut.30.12.1721), and as such, colonic specimens from patients with any history of inflammatory bowel diseases were not collected for the present study. As type 2 diabetes has been associated with impaired incretin response (10.2337/db07-0100), we did not collect colonic tissue from patients with diabetes for the current study. Human PBMCs were sourced under an agreement from the Australian Red Cross Blood service. Blood from 9 different individuals were used. No information is known on these individuals.

Recruitment

Participants recruited at Flinders medical centre and Flinders Private Hospital. Given that we did not select the patients based on any criteria other than those listed above (absence of IBD and diabetes) self-selection bias or other bias that might impact the results was not present.